MARIA S. MERIAN-Berichte

# LTER HAUSGARTEN 2018

## Long-Term Ecological Research in the Fram Strait

Cruise No. MSM77

September 15 – October 13, 2018
Longyearbyen (Svalbard) – Edinburgh (Scotland)

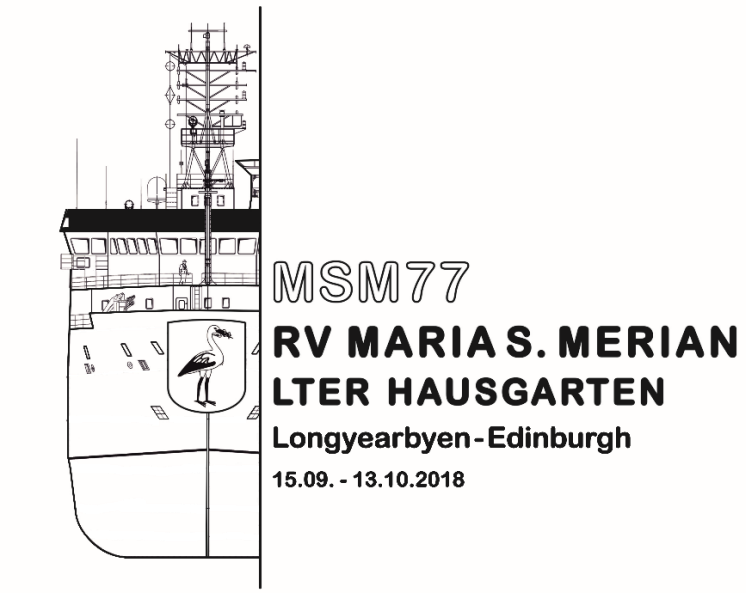


**T. Soltwedel, J. Bäger, J. Barz, M. Bergmann, M. Busack, M. Chikina, J. Hagemann, C. Hasemann, M. Hofbauer, U. Hoge, M. Iversen, M. Käß, T. Klüver, C. Konrad, S. Lehmenhecker, A. Nordhausen, I. Schewe, A. Sonnek, M. Tekman, A. von Jackowski, F. Wenzhöfer, T. Wulff**

Chief Scientist:
Dr. Thomas Soltwedel

Institution:
Alfred-Wegener-Institut Helmholtz-Zentrum für Polar- und Meeresforschung

# Table of Contents

## 1 Summary

The 77th cruise of the RV MARIA S. MERIAN contributed to various large national and international research and infrastructure projects (FRAM, ARCHES, INTAROS, ICOS, SIOS) as well as to the research programme PACES-II (Polar Regions and Coasts in the changing Earth System) of the Alfred-Wegener-Institute Helmholtz-Center for Polar and Marine Research (AWI). Investigations within Work Package 4 (Arctic sea ice and its interaction with ocean and ecosystems) of the PACES-II programme, aim at assessing and quantifying ecosystem changes from surface waters to the deep ocean in response to the retreating sea ice, and at exploring the most important (feedback) processes determining temporal and spatial variability. Contributions to the PACES-II Work Package 6 (Large scale variability and change in polar benthic biota and ecosystem functions) include the identification of spatial patterns and temporal trends in relevant benthic community functions, and the development of a comprehensive science community reference collection of observational data. Work carried out within WPs 4 and 6 will support the time-series studies at the LTER (Long-Term Ecological Research) observatory HAUSGARTEN (Fig. 1.1), where we document Global Change induced environmental variations on a polar deep-water ecosystem. This work is carried out in close co-operation between the HGF-MPG Joint Research Group on Deep-Sea Ecology and Technology and the PEBCAO Group (Phytoplankton Ecology and Biogeochemistry in the Changing Arctic Ocean) at AWI as well as the working group Microbial Geochemistry at the GEOMAR and the HGF Young Investigators Group SEAPUMP (Seasonal and regional food web interactions with the biological pump).

### Zusammenfassung

Die 77. Reise des FS MARIA S. MERIAN wurde genutzt, um Beiträge zu verschiedenen nationalen und internationalen Forschungs- und Infrastrukturprojekten (FRAM, ARCHES, INTAROS, ICOS, SIOS) sowie dem Forschungsprogramm PACES-II (Polar Regions and Coasts in the changing Earth System) des Alfred-Wegener-Instituts Helmholtz-Zentrum für Polar- und Meeresforschung (AWI) zu leisten. Im Arbeitspaket WP4 (Arctic sea ice and its interaction with ocean and ecosystems) des PACES-II Programms werden die mit dem Rückgang des Meereises verbundenen Ökosystem-Verschiebungen im Pelagial und im tiefen Ozean ermittelt und quantifiziert, und Rückkopplungsprozesse auf zeitliche und räumliche Prozesse untersucht. Unser Beitrag zum PACES-II Arbeitspaket WP6 (Large scale variability and change in polar benthic biota and ecosystem functions) beinhaltet die Identifizierung räumlicher und zeitlicher Entwicklungen in der Funktion ausgewählter Benthos-Gemeinschaften sowie den Aufbau eines umfassenden Repositoriums für Beobachtungsdaten. Die Arbeiten stellen einen weiteren Beitrag zur Sicherstellung der Langzeit-Beobachtungen am LTER (Long-Term Ecological Research) Observatorium HAUSGARTEN dar (Abb. 1.1), in denen der Einfluss von Umwelt-Veränderungen auf ein arktisches Tiefsee-Ökosystem dokumentiert wird. Diese Arbeiten werden in enger Zusammenarbeit der HGF-MPG Brückengruppe für Tiefsee-Ökologie und –Technologie und der PEBCAO-Gruppe (Phytoplankton Ecology and Biogeochemistry in the Changing Arctic Ocean) des AWI sowie der Arbeitsgruppe Mikrobielle Biogeochemie des GEOMAR und der HGF-Nachwuchsgruppe SEAPUMP (Seasonal and regional food web interactions with the biological pump) durchgeführt.

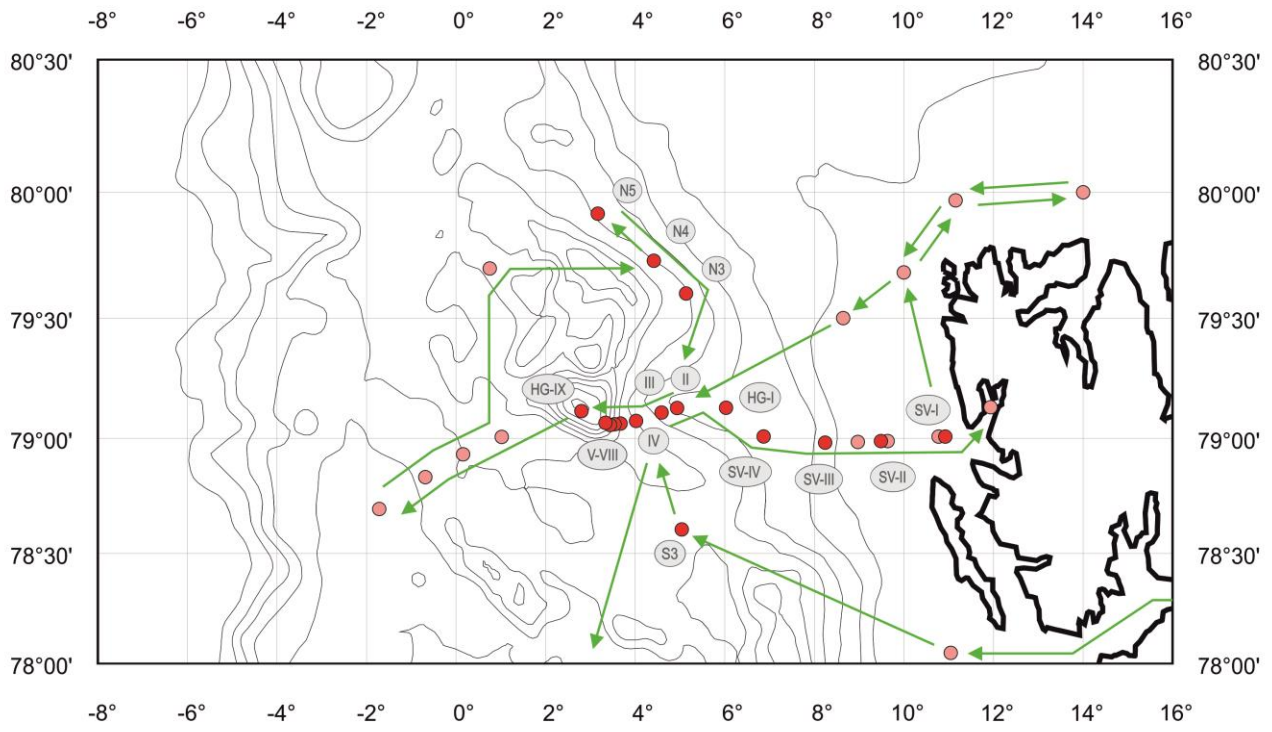


**Fig. 1.1** Stations sampled during RV MARIA S. MERIAN cruise MSM77 (red circles: permanent HAUSGARTEN sites; light-red circles: additional stations sampled during the expedition).

## 2 Participants

| | Name | Task | Institute |
|---|---|---|---|
| 1. | Dr. Thomas Soltwedel | Chief Scientist | AWI |
| 2. | Jana Bäger | Technician | AWI |
| 3. | Jakob Barz | Technician | MPIMM |
| 4. | Dr. Melanie Bergmann | Biologist | AWI |
| 5. | Michael Busack | Technician | AWI |
| 6. | Margarita Chikina | Biologist | IORAS |
| 7. | Jonas Hagemann | Technician | AWI |
| 8. | Dr. Christiane Hasemann | Biologist | AWI |
| 9. | Michael Hofbauer | Technician | AWI |
| 10. | Ulrich Hoge | Engineer | AWI |
| 11. | Dr. Morten Iversen | Biogeochemist | AWI |
| 12. | Melissa Käß | Biologist | AWI |
| 13. | Tania Klüver | Technician | GEOMAR |
| 14. | Christian Konrad | Technician | MARUM |
| 15. | Sascha Lehmenhecker | Engineer | AWI |
| 16. | Axel Nordhausen | Technician | MPIMM |
| 17. | Dr. Ingo Schewe | Biologist | AWI |
| 18. | Andreas Sonnek | Technician | MPIMM |
| 19. | Mine Tekman | Biologist | AWI |
| 20. | Anabel von Jackowski | Biogeochemist | AWI |
| 21. | Dr. Frank Wenzhöfer | Biogeochemist | AWI |
| 22. | Dr. Thorben Wulff | Engineer | AWI |

| | |
|---|---|
| AWI | Alfred-Wegener-Institut Helmholtz-Zentrum für Polar- und Meeresforschung<br>Am Handelshafen 12<br>27570 Bremerhaven |
| GEOMAR | GEOMAR Helmholtz-Zentrum für Ozeanforschung Kiel<br>Wischhofstr. 1-3<br>24148 Kiel |
| MARUM | MARUM – Zentrum für Marine Umweltwissenschaften<br>Löbener Str. 8<br>28359 Bremen |
| MPIMM | Max-Planck-Institut für Marine Mikrobiologie<br>Celsiusstr. 1<br>28359 Bremen |
| IORAS | P.P. Shirshov Institute of Oceanology, Russian Academy of Sciences<br>Nakhimovsky Pr., 36<br>117997 Moscow<br>Russia |

# 3 Research Program

## Impact of Climate Change on Arctic marine ecosystems

While always fluctuating, the global climate is presently experiencing a period of constantly increasing temperatures, with a warming trend amplified in the Arctic (Hassol, 2004). Results of large-scale simulations of the Earth's future climate by several global climate models predict a continuous increase in air and water temperatures, also leading to further reduction in ice-cover (IPCC, 2013). Since the 1950s, sea ice retreat in the Arctic Ocean has been relatively modest at rates of 3-4% per decade (Parkinson et al., 1999). However, since the late 1990s, annual-averaged shrinking rates accelerated to 10.7% per decade (Comiso et al., 2008), whilst the summer sea ice extent has shrunk even more rapidly. According to the US National Snow and Ice Data Center (NSIDC), arctic sea ice during the 2012 melt season has reached its lowest extent since satellites began measuring sea-ice in 1979, with 44% ice coverage below the 1981-2010 average, and 16% ice coverage below the previous minimum extent in 2007.

The shift from an ice-covered and cold ocean to an ice-free and warmer ocean will have severe impacts on the polar marine ecosystem and its functioning (e.g. Wassmann et al., 2011). Thinner ice may permit better growth of ice algae, but earlier and faster spring melting may reduce their growing season (Arrigo, 2013). Altered algal abundance and composition will affect zooplankton community structure (Caron & Hutchins, 2013) and subsequently the flux of particulate organic matter to the seafloor (Wohlers et al., 2009), where the changing quantity and quality of this matter will impact benthic communities (Kortsch et al., 2012; Jones et al., 2013). Changes in the predominance of certain trophic pathways will have cascading effects propagating through the entire marine community. Generally, arctic marine organisms will be compromised by temperature regimes approaching the limits of their thermal capacity (Burrows et al., 2011, 2014). As a consequence, warmer waters in the Arctic will allow a northward expansion of sub-arctic and boreal species (Hirche & Kosobokova, 2007; Poloczanska et al., 2013). Besides water temperature increase, expanding ocean acidification will pose another threat to pelagic and benthic life in the Arctic Ocean (e.g. Bates et al., 2009; Lischka & Riebesell, 2012; AMAP, 2013).

To detect and track the impact of large-scale environmental changes in the transition zone between the northern North Atlantic and the central Arctic Ocean, and to determine experimentally the factors controlling deep-sea biodiversity, the AWI established the LTER (Long-Term Ecological Research) observatory HAUSGARTEN (Soltwedel et al., 2005, 2016). Since 2014, this observatory is successively extended within the frame of the HGF infrastructure project FRAM (Frontiers in Arctic marine Monitoring) and covers currently 21 permanent sampling sites on the West-Spitsbergen and East-Greenland slope at water depths between 250 and 5500 m. Regular sampling as well as the deployment of moorings and different free-falling systems (bottom-lander), which act as local observation platforms, has taken place since the observatory was established back in 1999. The central HAUSGARTEN station at about 79°N, 04°E in the eastern Fram Strait (~2500 m water depth) serves as an experimental area for unique biological experiments at the deep seafloor, simulating various scenarios in changing environmental settings (Premke et al., 2006; Gallucci et al., 2008; Kanzog et al., 2009; Guilini et al., 2011; Soltwedel et al., 2013, 2017).

Time-series studies at the HAUSGARTEN observatory provide insights into processes and dynamics within an arctic marine ecosystem and act as a baseline for further investigations of ongoing changes in the Fram Strait. Long-term observations at HAUSGARTEN will significantly contribute to the global community's efforts to understand variations in ecosystem structure and functioning on seasonal to decadal time-scales in an overall warming Arctic and will allow for improved future predictions under different climate scenarios.

## 4 Narrative of the Cruise

The 77$^{th}$ cruise of the RV MARIA S. MERIAN started in the early evening of September 15$^{th}$ in Longyearbyen (Svalbard). During the first week of the expedition, we mainly operated in eastern parts of the Fram Strait between 77°00'N and 79°30'N, and between 03°00'E and 15°00'E. Water samples were taken using a CTD/Rosette Water Sampler, while particles in the water column were detected with a camera system and caught with a Marine Snow Catcher and a short drift-mooring equipped with sediment traps. A cabled photo/video system (Ocean Floor Observation System, OFOS) was towed at 1-2 m above seafloor to study large-scale distribution patterns of epi/megafauna organisms on the seafloor. Sediments were sampled by means of a TV-guided multicorer and a box corer. At the central HAUSGARTEN site (79°N, 04°E), we recovered a free-falling system (bottom-lander) and an autonomous benthic crawler system deployed during RV POLARSTERN expeditions PS107 and PS108, respectively, in summer 2017. Another bottom-lander equipped with incubation chambers and an oxygen microprofiler was deployed for about three days at the southernmost HAUSGARTEN site S3 to study remineralisation processes at the deep seafloor. An Autonomous Underwater Vehicle (AUV) was used for physico-chemical and biological surveys in the water column. The AUV was equipped with various sensors (e.g. CTD, ADCP, $CO_2$ and light sensors) and a water sampler. Steaming time between stations was repeatedly used for litter surveys registering floating debris at the sea surface.

During the second week of the cruise, we mainly operated in front of Kongsfjorden and off northeast and north Svalbard. Slightly impeded by the rather bad weather conditions, we continued our sampling programme in the water column and at the seafloor. On the shelf off north-western Svalbard, a bottom-lander equipped with incubation chambers and an oxygen microprofiler was deployed for about two days to study remineralisation processes at the deep seafloor. A second bottom-lander was deployed on the Vestnesa Ridge at about 1500 m water depth for a short-term test of a new experimental set-up to study effects of ocean acidification on benthic organisms. Our new autonomous benthic crawler NOMAD equipped with a microprofiler, benthic chambers and a camera system was deployed at the same site to test its performance. In-situ pumps attached to the CTD/Rosette Water Sampler cable were used at different water depths to detect microplastic particles in the water column. On the Svalbard shelf, the AUV was used close to the seafloor to test a new on-board multi-beam system.

During the third week we worked mainly in central and northern parts of the Fram Strait. Once again we used the entire range of instruments that we had with us on this expedition. The bottom-lander carrying the acidification experiment as well as the benthic crawler TRAMPER were deployed

for about one year at 1500 m and 2500 m, respectively, off Svalbard. The recovery of the two instruments is planned for the RV POLARSTERN cruise PS121 in summer 2019. Towards the end of the week we finally succeeded to recover our benthic crawler NOMAD, which we had deployed during the second week at 1500 m water depth on the Vestnesa Ridge off Spitsbergen. The crawler had persistently denied the dropping of its basic weight, so that the device could not independently return to the sea surface by its buoyancy. Therefore we decided to "fish" for the vehicle. For this we used our towed camera system OFOS, underneath we attached strong ropes with large hooks. Thanks to the incredible manoeuvrability of RV MARIA S. MERIAN, which enabled us to hold the ship exactly in position and move it precisely at meter-scales (!), the ship's command and the winch operator finally managed to "pick up" the device and bring it safely back to the sea surface.

On Saturday, October 5th, we set sail for Edinburgh. A short stop over south of Jan Mayen was done to successfully recover a malfunctioning Argo-Float for colleagues at the Euro-Argo Operations Centre. The expedition ended in the afternoon of October 12th.

# 5 Preliminary Results

## 5.1 Biogeochemical and Ecological Studies at the Deep Seafloor

(I. Schewe, J. Bäger, M. Bergmann, M. Chikina, C. Hasemann, U. Hoge, M. Käß)

During the RV MARIA S. MERIAN expedition MSM77 investigations of the deep-sea benthos were conducted at all HAUSGARTEN sites in eastern parts of the Fram Strait (Fig 5.1.1). HAUSGARTEN stations on the East-Greenland slope were not sampled as they were covered by sea-ice. However, in order to bridge the gap between the sites in eastern and western parts of the strait, we sampled three additional stations in the central Fram Strait with a multicorer (MUC) (DI - DIII), and four stations with a box corer (BC) (DI - DIV). Benthic investigations comprised biochemical analyses to estimate food availability at the seafloor and to determine benthic activity and biomass. Additional box corer samples were retrieved to study the ecological function of macrofauna communities on the Svalbard shelf compared to the deep Fram Strait.

- *Biogenic sediment compounds and meiofauna*

Virtually undisturbed sediment samples were taken using a multicorer (MUC). Various biogenic compounds from these sediments were analysed to estimate activities (i.e. bacterial exoenzymatic activity) and the total biomass (i.e. particulate proteins, phospholipids) of the smallest sediment-inhabiting organisms. Results will help to describe ecosystem changes in the benthal of the Arctic Ocean. Sediments retrieved by the MUC will also be analysed for the quantitative and qualitative assessment of the small benthic biota (meiofauna). The uppermost five centimetres of sediments, retrieved with the MUC, were sub-sampled to analyse parameters indicating the input of organic matter to the seafloor as well as sediment-bound biomass and benthic activity. Additional samples were taken to analyse the abundance and biomass of bacteria as well as meiofauna densities and the diversity patterns of nematodes. Sediment-bound chloroplastic pigments (chlorophyll *a* and its degradation products) represent a suitable indicator for the input of phytodetritus to the seafloor,

representing the major food source for benthic organisms. They can be analysed with high sensitivity by fluorometric methods. To estimate the potential heterotrophic activity of bacteria, we measured cleaving rates of extracellular enzymes using the model-substrate FDA (fluorescein-di-acetate) in incubation experiments. Bacterial activity and chloroplastic pigments were analysed on board. All other sub-samples were stored for later analyses of various biochemical bulk parameters at the home lab.

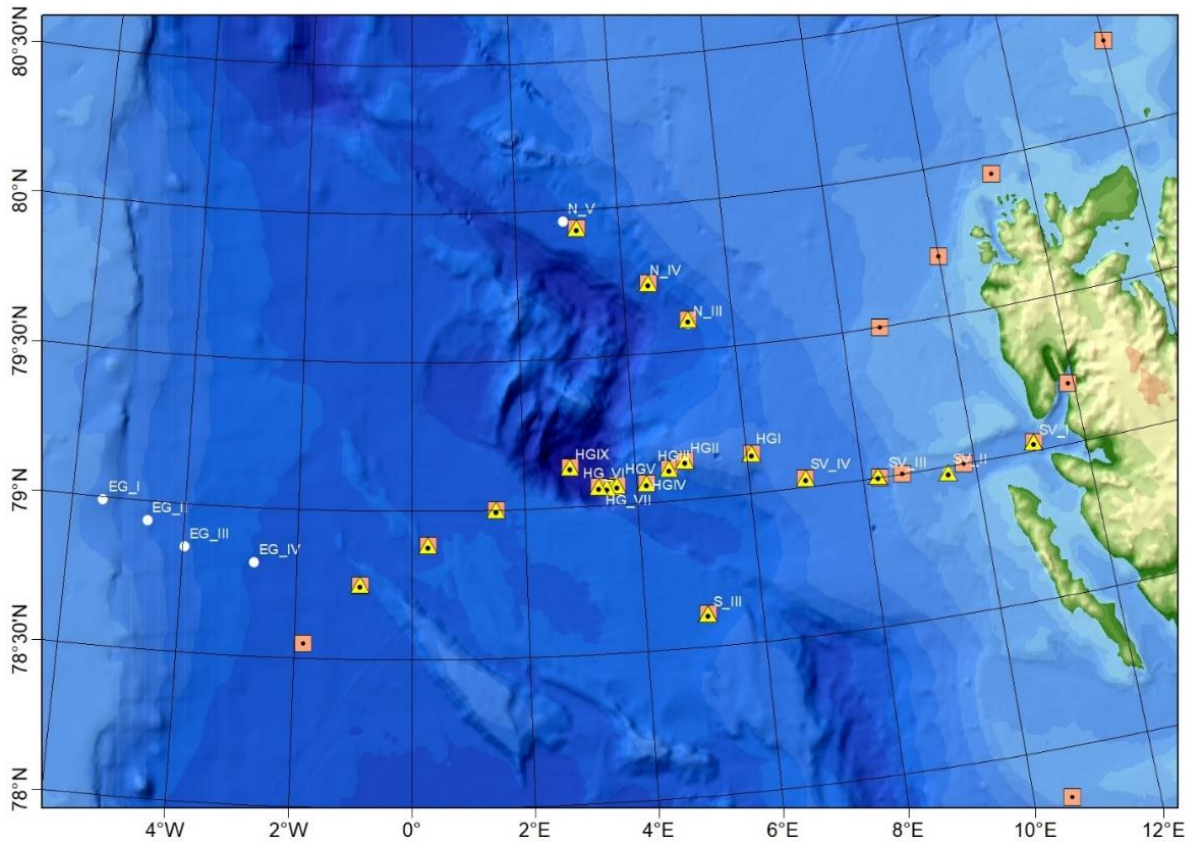


**Fig. 5.1.1** Benthic sampling sites during MSM77 (yellow triangles: MUC sampling, red squares: BC sampling).

Comparing the concentrations of sediment-bound pigments (Fig. 5.1.2 a) and the potential bacterial activity (Fig. 5.1.2 b) at four stations at 2500 m water depth along the latitudinal HAUSGARTEN transect (HG-IV, DI - DIII) we found conspicuous differences. All four stations exhibited generally decreasing values with increasing sediment depth. Steepest gradients were found at the westernmost station DIII, shallowest gradients occurred at station DI. Except from station DI, at all stations similarly high values for chloroplastic pigment concentrations (around 20 µg/ml) as well as for bacterial activity (around 6.0 nmol/ml·h$^{-1}$) occurred within the upper sediment layer (0-1 cm). At DI values in the upper sediment layer for both parameters were clearly lower (CPE: around 10 µg/ml and FDA: around 4.0 nmol/ml·h$^{-1}$) compared to the remaining stations. Stations DI - DIII were sampled the first time during MSM77, so the upcoming years must show whether this trend is confirmed.

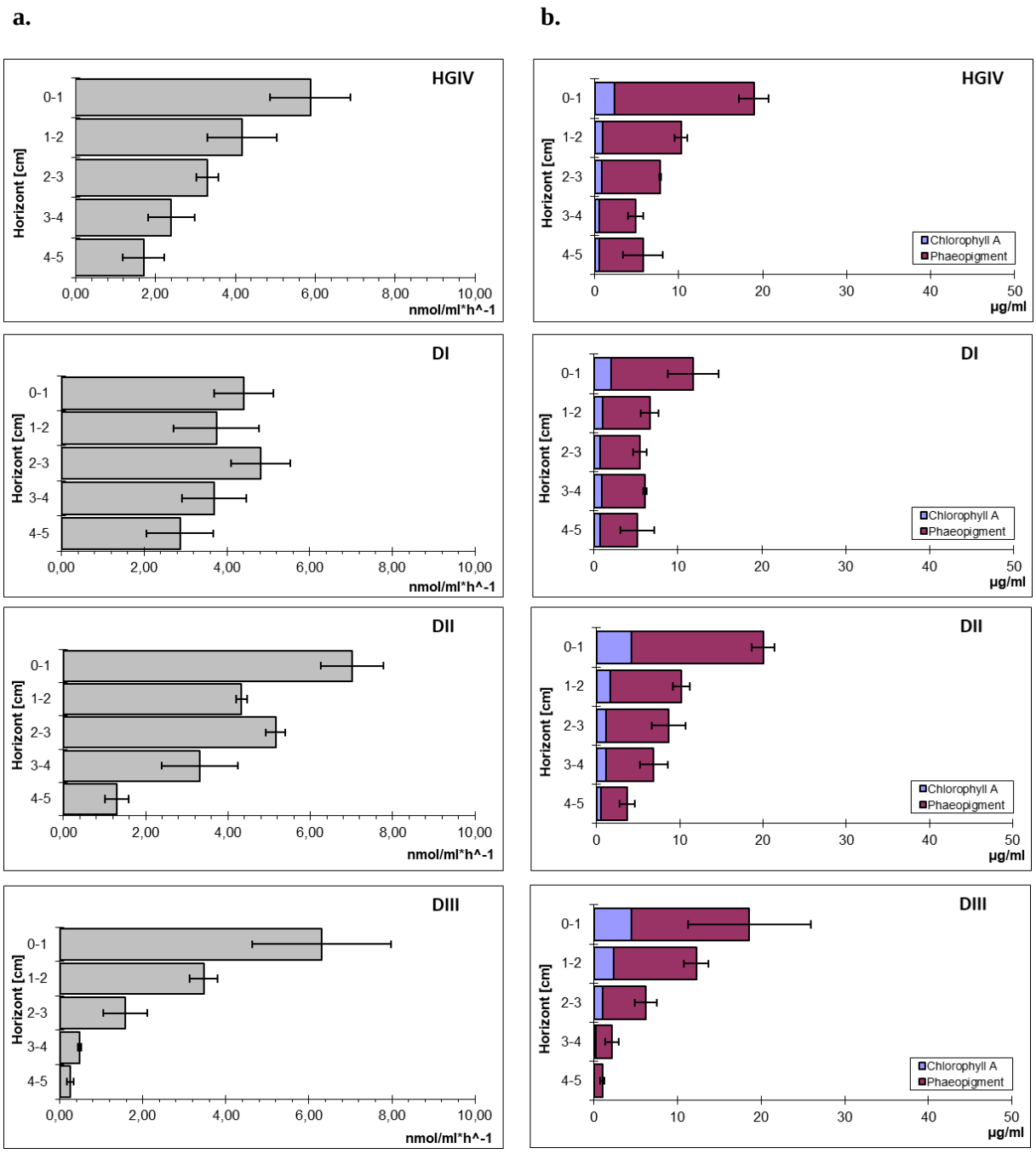


**Fig. 5.1.2** Hydrolytic activity of bacteria (FDA) (a) and sediment-bound chloroplastic pigments (b) in the upper five sediment centimetres of four stations along the latitudinal HAUSGARTEN transect at ~2500 m water depth.

- *Macrofauna sampling*

Sampling took place at the Svalbard shelf along a 150 m isobath as well as latitudinal across the Fram Strait ranging from the East Greenland continental margin to Kongsfjorden (Fig. 5.1.1). Shallow water stations <1000 m water depth were chosen and repeated according to RV HEINCKE expedition HE451.1 (11.-29.09.2015; Tromsø-Longyearbyen). The deep stations >1000 m water depth were chosen following previous studies of Wlodarska-Kowalczuk et al. (2004), Budaeva et al. (2008), Vedenin et al. (2016) and Käß et al. (*in prep.*). Stations were added to get a full latitudinal and longitudinal range accordingly.

A total of 29 stations were successfully sampled with an USNEL box corer covering an area of 0.25 $m^2$. Each box corer sample was divided into eight subsamples (pseudo replicates). The uppermost 12 cm of the sediment were chosen for analyses. Each subsample (3750 $cm^3$) was gently washed through a 0.5 mm mesh size sieve and fixed with 4% formalin. Fragile animals were removed from the sediment surface and fixed in 4% formalin before the sieving procedure.

- *Abundance and composition of megafauna*

Epibenthic megafauna inhabit the sediment-water interface and are traditionally described as those organisms that are visible in photographs and/or are >1.5 cm (Grassle et al.,1975; Rex, 1981). They play an important role in the deep-sea community as they influence benthic respiration, nutrient cycles and bioturbation, shape community structure through predation and also provide structure at the sediment-water interface. Thus, it is important to understand variations in the megafaunal community with depth, latitude, time and habitat features such as hard substrates. To assess megafaunal dynamics over time, we conduct camera surveys along the same transect positions (megafaunal time-series) (Bergmann et al., 2011; Meyer et al., 2013; Taylor et al., 2017; 2018).

A towed camera system (Ocean Floor Observation System, OFOS) was used for megafauna investigations. This method is non-invasive and allows us to gain *in situ* views of the organisms at a large-scale. The three transects visited during MSM77 were located at stations HG-I, HG-IV and S-3 (Table 5.1.1). The footage will be used to continue the image time-series. In addition, a time-lapse camera, fitted to a freefalling system (bottom-lander) was recovered and re-deployed. The bottom-lander had been at the seafloor of the central HAUSGARTEN station HG-IV for 1 year and had taken short videos twice a day. Analysis of this footage will allow us to assess changes at a higher temporal scale, e.g. seasonal changes.

The station HG-I (1200 m water depth) was characterised primarily by a host of brittlestars (*Ophiocten hastatum*) and worm tubes with some cerianthid anemones, pycnogonids (*Colloscendeis proboscidea*), eelpout fish (*Lycodes squamiventer*) and a few rays (*Amblyraja hyperboreus*). The two deeper stations (HG-IV, S3, approx. 2300-2600 m) had a different species composition with many sea cucumbers (*Elpidia heckeri*), feather stars (*Bathycrinus capenterii*), occasional sponges (*Cladorhiza gelida, Caulophacus arcticus*), shrimps (*Bythocaris* spp.) and the burrowing amphipod *Neohela lamia*. Results of the time-series analyses will only be available once the collected images will have been analysed. A few selected images and photographed species are shown in Figure 5.1.3.

**Table 5.1.1** Details of the OFOS casts.

| Station | Cast No. | Timestamp | Action | Latitude (N) | Longitude (E) | Depth (m) |
|---|---|---|---|---|---|---|
| S3 | MSM77_3-5 | 17.09.2018 03:41 | Start | 78°37.006' | 05°00.036' | 2313 |
| S3 | MSM77_3-5 | 17.09.2018 07:27 | End | 78°37.007' | 05°09.601' | 2300 |
| HG-I | MSM77_11-1 | 20.09.2018 01:18 | Start | 79°07.930' | 06°15.702' | 1289 |
| HG-I | MSM77_11-1 | 20.09.2018 04:26 | End | 79°08.017' | 06°07.423' | 1244 |
| HG-IV | MSM77_35-4 | 27.09.2018 17:44 | Start | 79°03.755' | 04°17.155' | 2365 |
| HG-IV | MSM77_35-4 | 27.09.2018 22:22 | End | 79°01.898' | 04°09.991' | 2575 |

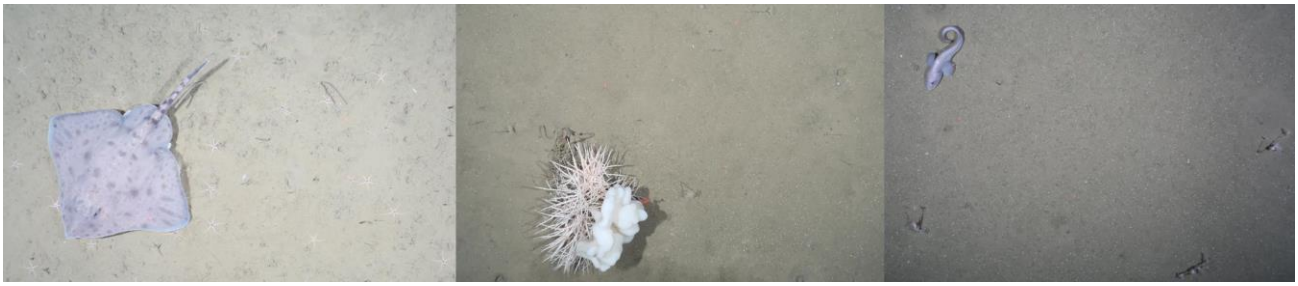

**Fig. 5.1.3** Images taken by Ocean Floor Observation System from (left to right) showing a ray *Amblyraja hyperborea* and brittle stars at HG-I, two species of sponges (*Cladorhiza gelida*, *Caulophacus arcticus*) at HG-IV, and the eelpout fish *Lycodes frigidus* and feather stars (*Bathycrinus capenterii*) at S3.

## 5.2 Biogeochemical and Ecological Studies in the Water Column

(A. von Jackowski, J. Barz, T. Klüver;
E.-M. Nöthig, A. Engel, K. Metfies, C. Bienhold, *not on board*)

The project PEBCAO (Plankton Ecology and Biogeochemistry in a Changing Arctic Ocean) focusses on the plankton community and the microbial processes relevant for biogeochemical cycles of the Arctic Ocean. This research focus is acknowledging that the Arctic Ocean has gained increasing attention over the past years because of the drastic decrease in sea ice and increase in temperature, which is about twice as fast as the global mean rate. In addition, the chemical equilibrium and the elemental cycling in the surface ocean will alter due to ocean acidification. These environmental changes will have consequences for the biogeochemistry and ecology of the Arctic pelagic system. The effects of changes in the environmental conditions on the polar plankton community can only be detected through long-term observation of the species and processes. Our studies on plankton ecology have started in 1991, and since 2009 sampling has been significantly intensified by the PEBCAO group in the Fram Strait at ~79°N. Since then, our studies are based on combining a broad set of parameters. This includes classical bulk measurements and microscopy, optical measurements and satellite observations, molecular genetic approaches, and cutting edge methods for zooplankton observations to study plankton ecology in a holistic approach. Since 2014, the PEBCAO group is

related to the FRAM (Frontiers in Arctic Monitoring) Ocean Observatory Team providing ground truthing information for water column monitoring of plankton ecological, biogeochemical parameters and microbial (prokaryotic and eukaryotic) biodiversity.

Over the past nine years, we have compiled complementary information on annual variability in phytoplankton composition, primary production, bacterial activity and zooplankton composition (Nöthig et al., 2015). Previous assessments in the study area indicated that the protist composition in the West Spitsbergen Current changed in the summer months. A dominance of diatoms was replaced by a dominance of *Phaeocystis pouchetii* and other small pico- and nanoplankton species. Our recent regular annual observations in Fram Strait suggest that TEP concentrations in the water column could be correlated with the *P. pouchetii* abundance (Engel et al., 2017). These data were complemented by our molecular genetic investigations that provided new insights into eukaryotic microbial community composition with special emphasis on the contribution of pico-eukaryotes to plankton communities (Metfies et al., 2016).

Sampling for the FRAM project usually occurs in the scope of annual summer cruises in July/August. This year, we planned for an additional cruise to investigate the bloom degradation in the fall, which was in focus of the RV MARIA S. MERIAN expedition MSM77.

- *Biogeochemistry and phytoplankton*

Climate induced changes will impact the biodiversity in pelagic ecosystems. At the base of the food web, we expect small algae to gain more importance in mediating element and matter turnover as well as matter and energy fluxes in future Arctic pelagic systems. In order to examine changes, including the smallest fractions, molecular methods are applied to complement traditional microscopy. The characterization of the communities with molecular methods is independent of cell-size and distinct morphological features. The assessment of the biodiversity and biogeography of Arctic phytoplankton will be based on the analysis of ribosomal genes with next generation sequencing technology. Besides molecular methods the set of parameters investigated includes classical bulk measurements (e.g. chlorophyll *a*, POC/N) and microscopy.

- *Bacterioplankton*

As part of the FRAM project, we aim to investigate the bacterial activity and diversity, as polar regions are also characterized by strong phytoplankton blooms in late spring to early summer. The decay of such blooms has been well documented for the North Sea around Helgoland in recent years, but is still challenging to follow in polar regions. The bacterial fraction of the bloom is measured based on incubation experiments and molecular tools. The molecular toolkit covers sequencing approaches as well as Fluorescent In-Situ Hybridization (FISH) microscopy to allow a quantitative analysis. The molecular samples serve the continuation of observations of the diversity of microbial communities (Fadeev et al., *under review*) in the framework of the FRAM project.

Samples for a large variety of parameters have been collected in the area of the LTER observatory HAUSGARTEN located in the Fram Strait, including the frontal zone separating the warm and cold water masses originating from the West Spitsbergen Current and the East Greenland Current. Sampling as accomplished by the PEBCAO team from CTD casts are summarized in the Tables 5.2.1 and 5.2.2.

**Table 5.2.1** Biogeochemical parameters sampled from CTD casts (Chl *a*: chlorophyll *a*; POC/PON: particulate organic carbon and nitrogen; DOC: dissolved organic carbon; TDN: total dissolved nitrogen; TEP: transparent exopolymer particles; CSP: Coomassie-stainable particles; TA: total alkalinity; DCHO: carbohydrates; AA: amino acids; "x" indicates that measurement was taken, whereas "o" indicates that it was omitted).

| Station | CTD cast | Chl *a* | POC / PON | DOC / DON/ DOP/ DCHO | AA | TEP/ CSP | TA/DIC | Nutrients |
|---|---|---|---|---|---|---|---|---|
| SV-I | MSM77_24-1 | x | x | x | x | x | x | x |
| SV-II | MSM77_22-1 | x | x | x | x | x | o | x |
| SV-III | MSM77_19-1 | x | x | x | x | x | o | x |
| SV-IV | MSM77_17-1 | x | x | x | x | x | x | x |
| NSB-1 | MSM77_29-1 | x | x | x | x | x | o | x |
| HG-I | MSM77_13-1<br>MSM77_13-4 | x<br>o | x<br>x | x<br>x | x<br>x | x<br>x | o<br>o | x<br>x |
| HG-II | MSM77_12-1 | x | x | x | x | x | x | x |
| HG-III | MSM77_8-1 | x | x | x | x | x | x | x |
| HG-IV | MSM77_4-3 | x | x | x | x | x | x | x |
| HG-V | MSM77_36-1 | x | x | x | x | x | x | x |
| HG-VI | MSM77_6-1 | x | x | x | x | x | o | x |
| HG-VII | MSM77_37-1 | x | x | x | x | x | o | x |
| HG-VIII | MSM77_40-1 | x | x | x | x | x | o | x |
| HG-IX | MSM77_41-1 | x | x | x | x | x | x | x |
| D1 | MSM77_44-1 | x | x | x | x | x | o | x |
| D2 | MSM77_48-1 | x | o | x | x | x | o | x |
| D3 | MSM77_47-1 | x | o | x | x | x | o | x |
| D4 | MSM77_45-1<br>MSM77_46-4 | x<br>o | x<br>x | x<br>x | x<br>x | x<br>x | x<br>o | x<br>x |
| N5 | MSM77_52-1 | x | x | x | x | x | x | x |
| N4 | MSM77_53-1<br>MSM77_53-3 | x<br>o | x<br>x | x<br>x | x<br>x | x<br>x | o<br>o | x<br>x |
| N3 | MSM77_54-1 | x | x | x | x | x | x | x |
| S3 | MSM77_3-1 | x | x | x | x | x | x | x |

**Table 5.2.2** Biological parameters sampled from CTD casts ("x" indicates that sample was taken, whereas "o" indicates that it was omitted).

| Station | CTD Cast | Phyto-plankton/ Bacterial cell no. | Bacterial biomass production | PP | Eukaryotic Abundance | Eukaryotic and Bacterial DNA | FISH Bacteria |
|---|---|---|---|---|---|---|---|
| SV-I | MSM77_24-1 | x | x | x | x | x | x |
| SV-II | MSM77_22-1 | x | x | o | x | x | x |
| SV-III | MSM77_19-1 | x | x | o | x | x | x |
| SV-IV | MSM77_17-1 | x | x | x | x | x | x |
| NSB_1 | MSM77_29-1 | x | x | o | x | x | x |
| HG-I | MSM77_13-1 | x | x | o | x | x | x |
| | MSM77_13-4 | x | o | o | x | x | x |
| HG-II | MSM77_12-1 | x | x | x | x | x | x |
| HG-III | MSM77_8-1 | x | x | x | x | x | x |
| HG-IV | MSM77_4-3 | x | x | x | x | x | x |
| HG-V | MSM77_36-1 | x | x | x | x | x | x |
| HG-VI | MSM77_6-1 | x | x | o | x | x | x |
| HG-VII | MSM77_37-1 | x | x | o | x | x | x |
| HG-VIII | MSM77_40-1 | x | x | o | x | x | x |
| HG-IX | MSM77_41-1 | x | x | x | x | x | x |
| D1 | MSM77_44-1 | x | x | o | x | x | x |
| D2 | MSM77_48-1 | x | x | o | x | x | x |
| D3 | MSM77_47-1 | x | x | o | x | x | x |
| D4 | MSM77_46-4 | x | x | x | x | x | x |
| | MSM77_45-1 | x | o | o | x | x | x |
| N5 | MSM77_52-1 | x | x | x | x | x | x |
| N4 | MSM77_53-1 | x | x | o | x | x | x |
| | MSM77_53-3 | x | o | o | x | x | x |
| N3 | MSM77_54-1 | x | x | x | x | x | x |
| S3 | MSM77_03-1 | x | x | x | x | x | x |

Seawater samples were taken at a minimum of five depths by a CTD/Rosette Water Sampler (Fig. 5.2.1) to determine the impact of microbial processes on organic matter cycling. Sampling was conducted within the euphotic zone and at deeper layers at specific stations (S3, HG-I, N4). All stations were sampled at the surface (5 m), above deep chlorophyll maximum (DCM), the DCM, below DCM and 100 meter. The water from the CTD/Rosette Water Sampler was filtered for analysing biogeochemical parameters such as chlorophyll *a* (unfractionated); total, dissolved and particulate organic carbon (TOC, DOC, and POC); total, dissolved and particulate organic nitrogen (TN, DON, and PON), dissolved carbohydrates (DCHO), amino acid (AA) composition and nutrients (Table 5.2.1). All samples were preserved, refrigerated or frozen at -20°C or -80°C for storage until analyses in the home laboratories (AWI, GEOMAR). Concentrations of the dissolved substances will

be determined by the use of IC and HPLC at GEOMAR in Kiel. Furthermore, samples for transparent exopolymer particles (TEP) and Coomassie-stainable particles (CSP) were taken and stored at -20°C until analysis by photometry and microscopy in the home laboratory.

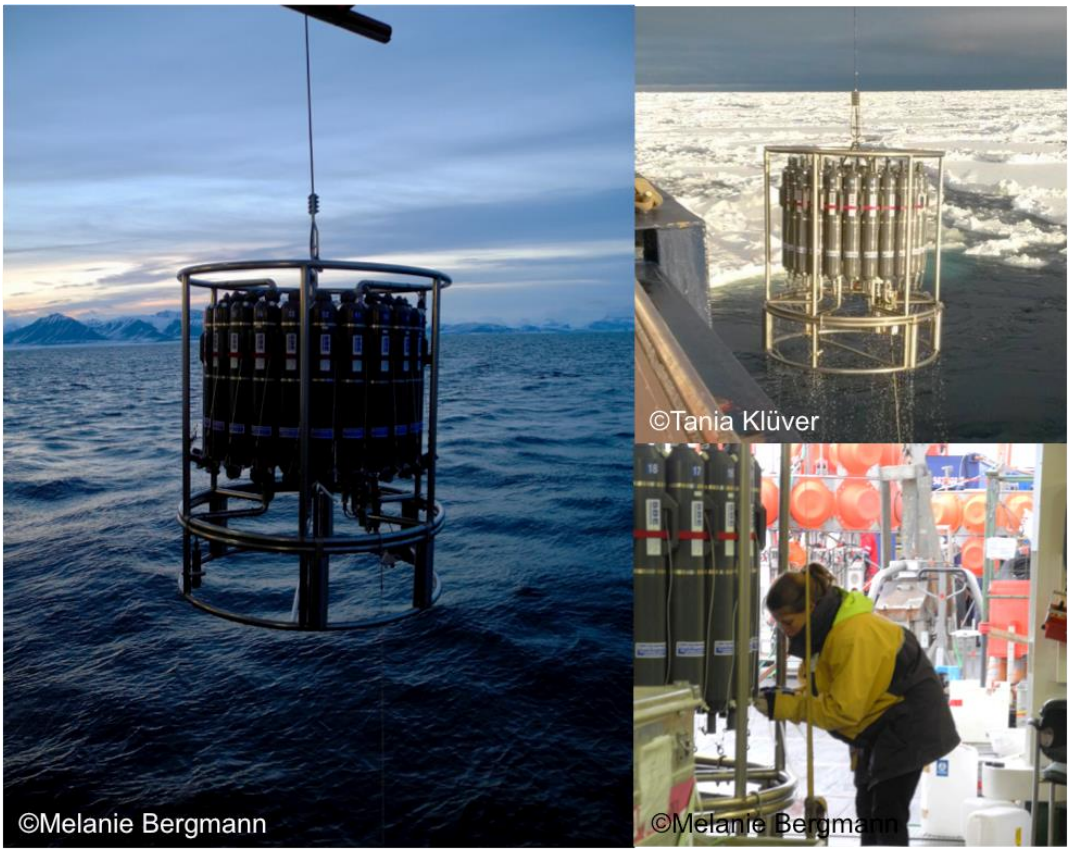


**Fig. 5.2.1** CTD/Rosette Water Sampler deployment during MSM77; Left: sampling at HAUSGARTEN station SV-II off Svalbard on 23.09.2018. Top right: CTD deployment at station D4 close to the ice edge in western parts of the Fram Strait on 1.10.2018; Bottom right: water subsampling from the CTD bottle.

Multiple methods will be applied to determine the phytoplankton and bacterial abundances and growth rates. Abundance will be determined using flow-cytometry as well as microscopic methods. Phytoplankton $^{14}C$ primary production was determined according to (Engel et al., 2013). Polycarbonate bottles were filled with 300 mL pre-filtered (mesh size 200 µm) sample and spiked with $NaH^{14}CO_3$ solution. Duplicated samples were incubated for 24 h at different light intensities (5, 45, 100 µE $cm^{-2}$ $s^{-1}$) and in darkness (blanks) at the temperature of the sea surface. Incubations were stopped by filtration onto 0.4 µm polycarbonate filters. Primary production of POC (PPPOC) was determined from material collected on the filter, while the filtrate was used to determine primary production of DOC (PPDOC). Bacterial growth rates were determined using the radioactive isotope approach of $^3H$ leucine, incubation time was 6 h (Simon & Azam, 1989).

To characterize the diversity of microbes present in the photic zone, water samples were taken from the CTD/Rosette Water Sampler (Table 5.2.2). Fractionated filtrations using pore sizes of 10.0, 3.0, and 0.4 µm were then conducted for microbial eukaryotic 18S rRNA gene sequencing. Samples were filtered on Sterivex filters (0.2 µm) for bacterial/archaeal 16S RNA gene analyses. Additionally, aliquots of seawater were preserved and filtered for visualization and quantification of specific microbial groups by Fluorescence In-Situ Hybridization (FISH). Filters were stored frozen at -20°C or -80°C.

All samples will be analysed in the home laboratories at AWI in Bremerhaven (biogeochemical parameters, phytoplankton abundance and molecular biology, zooplankton community composition and distribution), at GEOMAR in Kiel (biogeochemical parameters [DOC/DON/DOP, DCHO, AA, TEP/CSP], phytoplankton/bacterial growth rates), and MPIMM in Bremen (bacterioplankton community composition).

## 5.3 Pelagic Food-Web Interactions with the Biological Pump

(M. Iversen, C. Konrad)

Anthropogenic activities have increased atmospheric carbon dioxide ($CO_2$) levels to above 400 ppm, higher than at any point during the past 2 to 5 million years. Small sinking particles in the ocean are paramount for the control of carbon dioxide removal from the atmosphere and into the ocean. This is because the formation of sinking aggregates from photosynthetic plankton moves carbon from the surface to the deep ocean, which allows for further uptake of atmospheric carbon dioxide by the ocean. In this way, the oceans have the capacity to sequester large amounts of atmospheric $CO_2$ by exporting biologically fixed carbon to the deep ocean. The sinking aggregates also feed life below the ocean's surface sustaining the biomass of deep sea fish and other organisms and determine sediment formation on the seafloor. However, most of the organic matter produced by photosynthetic plants in the surface ocean is eaten by small animals or degraded by bacteria before it sinks deeper than 100 meters. This means that the carbon dioxide is only removed from the atmosphere for a few weeks before it is outgassed from the ocean again. The particles need to sink below 1000 m water depth to be removed from the atmosphere for more than 1000 years and only those particles reaching the seafloor will have their organic matter stored for millennia. Unfortunately, we know very little about processes that remove and transform the particles as they sink through the water column and, hence, the sequestration of atmospheric carbon dioxide in the world's oceans is only poorly understood.

The main objective during the cruise was to study the controlling mechanisms for attenuation and export of organic carbon flux through the water column. This was done by detailed investigations of particle dynamics in relations to plankton community structure and aggregate composition. We combined large and small scales, i.e. on a whole water perspective using *in situ* optics and drifting traps and direct measurements on individual aggregates collected *in situ* using Marine Snow Catchers.

We performed deployments and recoveries of drifting trap arrays and used a combination of different optical, biological, and physical sensors to capture particle processes through the water column. These studies were accompanied by laboratory experiments to investigate specific

mechanisms responsible for *in situ* carbon turnover within marine settling aggregates. These studies were done on *in situ* collected material (using the Marine Snow Catcher) to measure microbial degradation, aggregate size, composition, structure, and sinking velocities. The vertically changing particle concentrations and size distribution determined with the *in situ* optical systems can be used to derive high resolution carbon fluxes and remineralisation rates in various depth ranges. These high resolution carbon fluxes will enable determinations of bacterial degradation rates and consumption rates of aggregates due to zooplankton flux feeding.

- *Drifting Sediment Traps*

We used an array of free-drifting sediment traps to measure the export fluxes at 50 m, 100 m, 200 m, and 300 m depth (Fig. 5.3.1, Table 5.3.1). Each collection depth had a trap station that consisted of four cylindrical collection tubes with a gyroscopical attachment (Fig. 5.3.1). Three of the four collection cylinders at each depth were used to collect samples for biogeochemical measurements of total dry weight (DW), particulate organic carbon (POC), particulate organic nitrogen (PON), particulate inorganic carbon (PIC), and silica. The fourth trap cylinder at each depth was equipped with a viscous gel that preserved the structure, shape and size of the fragile settling particles (Fig. 5.3.2). After recovery of the drifting trap, the samples for bulk fluxes were frozen for later analysis in the home laboratory. The particles collected in the gel traps were photographed with a digital camera on board and frozen for further detailed investigations in the home laboratory. The image analyses of the gel traps will be used to determine the composition, abundance and size distribution of the sinking particles.

We deployed the drifting trap four times during the cruise. The drifting array consisted of a surface buoy equipped with an Iridium satellite unit that provided trap positions every 10 minutes with a resolution of two minutes. We used two Teledyne Benthos™ floats for buoyancy and 14 small buoyancy balls were placed between the surface buoy and the two benthos floats to act as wave breakers and thereby reducing the hydrodynamic effects on the sediments traps. The trap cylinders were mounted to a sediment station with gimbal mounts ensuring that they were maintaining a vertical position in the water column. Each cylinder was 1 m tall and had a diameter 10.4 cm, which resulted in a collection area of 84.95 $cm^2$.

**Fig. 5.3.1** Free-drifting sediment trap during deployment with one of the trap stations with the four trap cylinders.

**Table 5.3.1** Deployments of the free-drifting sediment trap with information about station name, date of deployment, time for deployment and recovery, latitude and longitude for deployment and recovery, as well as trap identification and deployment depths.

| Station name | Date | Time (UTC) | Latitude | Longitude | Trap name: deployment depths |
|---|---|---|---|---|---|
| MSM77_4-10 | 18.09.2018 | 05:55 | 79°04.832'N | 04°06.781'E | Deployment FDF15: 100, 200, and 400 m |
| MSM77_4-10 | 19.09.2018 | 11:02 | 79°03.928'N | 04°18.464'E | Recovery FDF15 |
| MSM77_21-1 | 22.09.2018 | 18:38 | 78°59.994'N | 08°14.962'E | Deployment FDF16: 50, 100, and 400 m |
| MSM77_21-1 | 26.09.2018 | 13:30 | 78°59.150'N | 08°10.611'E | Recovery FDF16 |
| MSM77_38-1 | 28.09.2018 | 13:20 | 79°07.850'N | 02°50.340'E | Deployment FDF17: 50, 100, and 400 m |
| MSM77_38-1 | 30.09.2018 | 09:50 | 78°58.801'S | 03°29.314'E | Recovery FDF17 |
| MSM77_50-1 | 03.10.2018 | 16:24 | 79°44.127'N | 04°28.962'E | Deployment FDF18: 50, 100, and 400 m |
| MSM77_50-1 | 04.10.2018 | 16:34 | 79°39.058'N | 04°32.504'E | Recovery FDF18 |

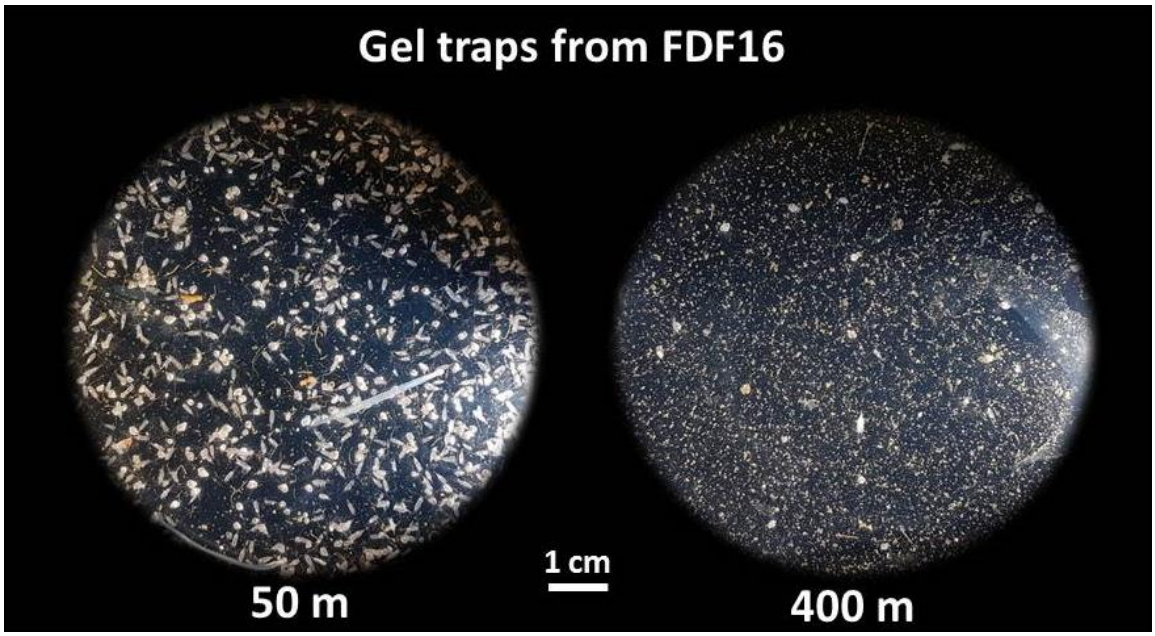


**Fig. 5.3.2** Examples of the particles collected in the gel traps at 50 m and 400 m during the FDF16 deployment.

We deployed drifting trap FDF15 at station HG-IV, FDF16 at station SV-III, FDF17 at station HG-IX, and FDF18 at station N4 (Fig. 1.1). All trap deployments were equipped with gel traps. The majority of the collected aggregates were heavily degraded mucous aggregates composed of unidentified minerals, presumably biominerals. Often copepod faecal pellets were abundant as well. We observed many pteropods with both the *in situ* optical systems and the sediment traps. The pteropod *Limacina* was the most abundant while the pteropod *Clione* was less frequently observed. It is likely that the aggregates were formed from discarded feeding mucous nets produced by *Limacina*.

Unfortunately we had to leave the FDF16 deployment in the water for almost four days, which resulted in many swimmers in the gel traps and rendering them difficult to use for particle analyses. However, it clearly illustrated the high abundance of *Limacina* at 50 m and copepods at 100 m (not shown), while at 400 m we mainly observe heavily degraded aggregates and only a few *Limacina*.

*Limacina* was the dominant zooplankton at stations SV-III, HG-IX, and N4 (Fig. 1.1) in the upper 50 m of the water column and the dominant particles observed at these stations were marine snow formed from mucous, presumably from the mucous feeding webs of *Limacina*. At HG-IV copepods were dominating the zooplankton community and the faecal pellets dominated the aggregates in the gel traps at 100 m, 200 m, and 400 m. We will perform detailed image analyses of the gel traps back in the home laboratory. We will also make biogeochemical analyses to determine mass fluxes of dry material, organic carbon, organic nitrogen, inorganic carbon, silicate, and lithogenic material.

- *Vertical profiles with the In Situ Camera and the DriftCam system*

The In Situ Camera (ISC) consisted of an industrial camera with removed infrared filter (from Basler) with backend electronics for timing, image acquisition and storage of data and a fixed focal length lens (16 mm Edmund Optics). Furthermore a DSPL battery (24 V, 38 Ah) was used to power the system (Fig. 5.3.3).

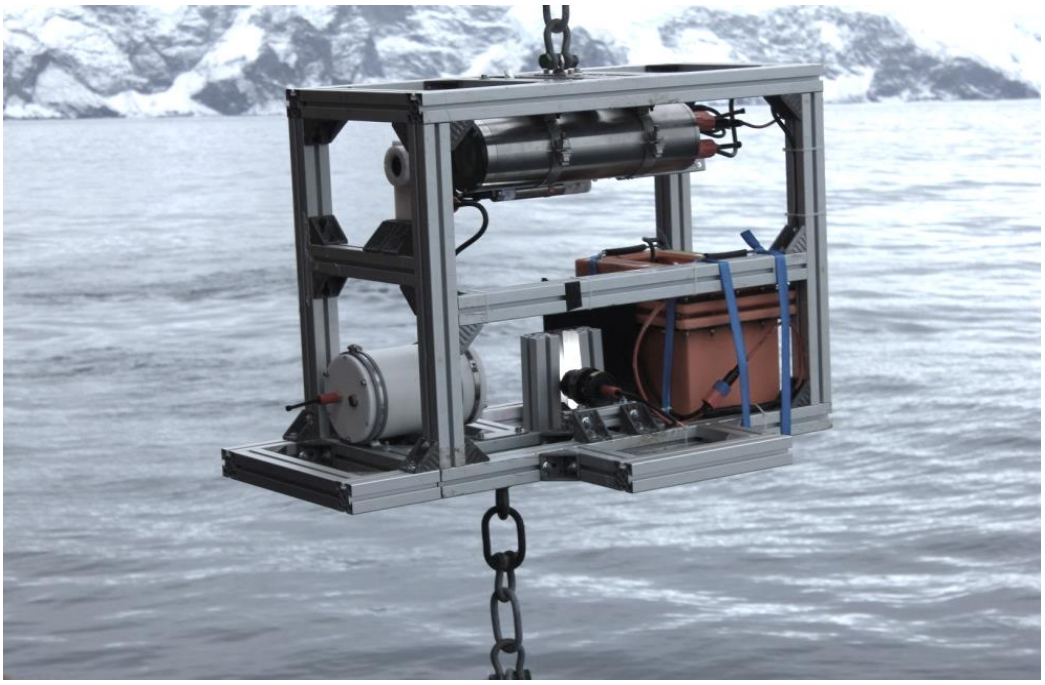

**Fig. 5.3.3** Deployment of the camera system platform equipped with the In Situ Camera (ISC), the DriftCam, and a Seabird SBE19 CTD.

A single board computer was both used as the operating system for the infrared camera and to acquire the images from the camera and send them to a SSD hard drive where they were stored. The illumination was provided by a custom made light source that consisted of infrared LEDs which were placed in an array in front of the camera. The choice of the infrared illumination was done to avoid disturbing the zooplankton that potentially would feed on the settling particles. With this geometrical arrangement of the camera and the light source we obtained shadow images of particles through the water column. We captured two images per second and lowered the ISC with 0.3 meters per second (lowest possible speed of winch).

The DriftCam consists of a Canon EOS 600D DSLR (18 Megapixel resolution) with an EF 50.2 macro-lens connected to a Canon Speedlight 430 EX II flash. Camera and flash were installed each in a POM pressure housing with a depth rating of 500 m. The camera could be programmed by using a Delamax LCD Timer, which allows time-lapse exposures at given intervals. The flash was mounted perpendicular to the optical axis of the camera at a distance of approx. 30 cm.

Both camera systems were mounted on the same platform together with a Seabird SBE19 CTD equipped with an oxygen sensor, a turbidity sensor, and a fluorescence sensor (Fig. 5.3.3). However, we had some issues with the flash housing and the DriftCam was therefore not mounted during all deployments of the camera platform.

We made 18 vertical profiles with the camera platform (Table 5.3.2). All profiles were equipped with the ISC, DriftCam, and the Seabird SBE19 CTD to get correlations of depth and images. During the whole cruise all three instruments were used in standalone mode and data was then afterwards correlated with Matlab according to the time-stamp of the images and the time of the CTD.

**Table 5.3.2** List of stations where the In Situ Camera (ISC) was deployed in the profiling mode.

| Profile No. | Station No | Date | Start Time (UTC) | Latitude | Longitude | Profile depth (m) |
|---|---|---|---|---|---|---|
| 1 | MSM77_3-4 | 17.09.2018 | 00:50:55 | 78°36.988'N | 05°04.085'E | 500 |
| 2 | MSM77_4-5 | 17.09.2018 | 18:30:32 | 79°03.551'N | 04°12.015'E | 500 |
| 3 | MSM77_4-11 | 18.09.2018 | 06:56:21 | 79°04.993'N | 04°05.544'E | 500 |
| 4 | MSM77_9-1 | 19.09.2018 | 11:53:35 | 79°03.964'N | 04°18.443'E | 500 |
| 5 | MSM77_13-3 | 20.09.2018 | 16:59:40 | 79°08.003'N | 06°05.544'E | 500 |
| 6 | MSM77_17-4 | 21.09.2018 | 23:42:06 | 79°01.801'N | 06°59.886'E | 500 |
| 7 | MSM77_21-3 | 22.09.2018 | 19:56:34 | 79°00.221'N | 08°16.847'E | 500 |
| 8 | MSM77_22-3 | 23.09.2018 | 01:12:13 | 78°58.809'N | 09°30.841'E | 200 |
| 9 | MSM77_27-1 | 23.09.2018 | 18:12:00 | 79°42.083'N | 10°00.057'E | 140 |
| 10 | MSM77_28-1 | 23.09.2018 | 21:29:19 | 79°56.490'N | 11°15.575'E | 120 |
| 11 | MSM77_29-2 | 24.09.2018 | 02:42:16 | 80°18.007'N | 13°59.954'E | 70 |
| 12 | MSM77_34-1 | 26.09.2018 | 14:20:54 | 78°59.150'N | 08°10.611'E | 500 |
| 13 | MSM77_38-2 | 28.09.2018 | 14:05:55 | 79°07.826'N | 02°49.540'E | 500 |
| 14 | MSM77_41-2 | 30.09.2018 | 10:35:20 | 78°58.820'N | 03°29.115'E | 500 |
| 15 | MSM77_46-2 | 01.10.2018 | 16:22:40 | 78°32.948'N | 01°50.205'W | 500 |
| 16 | MSM77_52-3 | 04.10.2018 | 00:33:50 | 79°56.285'N | 03°11.758'E | 500 |
| 17 | MSM77_53-6 | 04.10.2018 | 17:23:20 | 79°39.069'N | 04°31.708'E | 500 |
| 18 | MSM77_54-3 | 04.10.2018 | 20:24:00 | 79°36.233'N | 05°10.369'E | 500 |

We obtained vertical profiles of particle abundance and size-distribution through the water column. We still need to analyse the images, but the first glance at a profile obtained at station HG-IV (Fig. 5.3.4) showed higher abundance of aggregates with diameters between 100 µm and 200 µm in the upper 50 m of the water column. At depths below 50 m the particle and aggregate abundance remained low and quasi constant. The camera profiles further allow identifications of different particle types and sizes at specific depths and times.

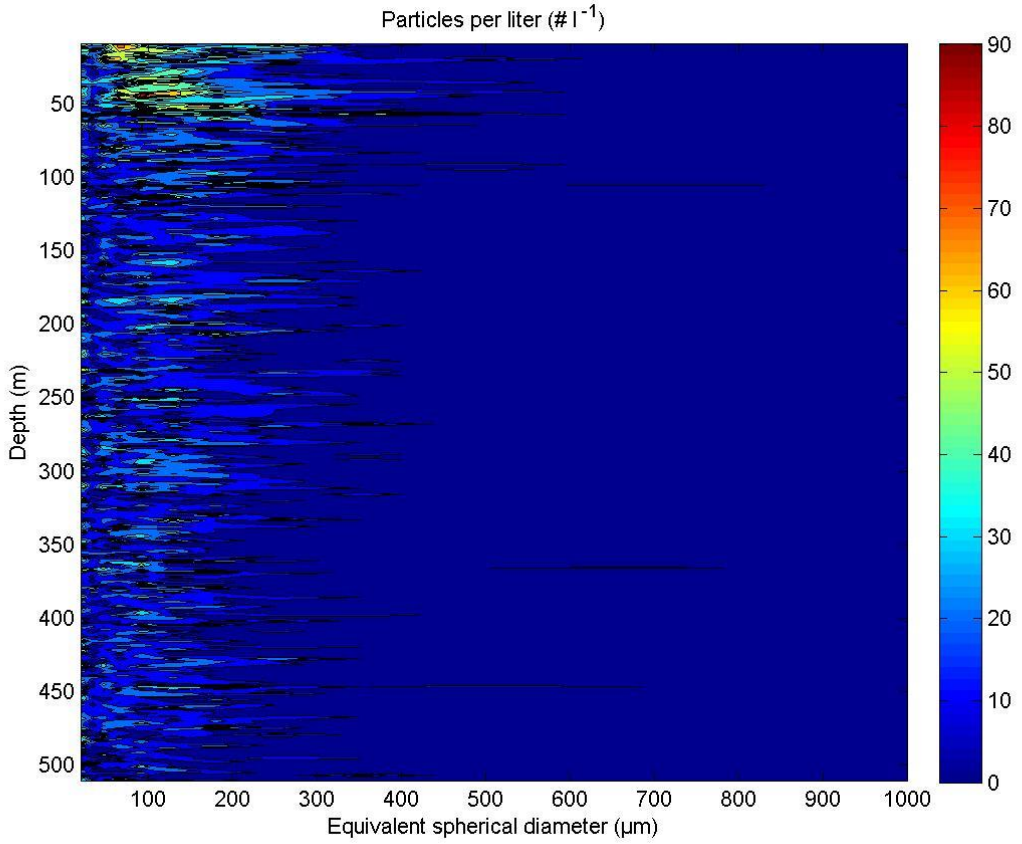


**Fig. 5.3.4** Example of an ISC profile down to 500 m water depth at the central HAUSGARTEN site HG-IV. The plot shows number of particles of different sizes per litre through the water column.

- *ROSINA - Remotely Observing In-situ Camera for Aggregates*

The newly developed *in situ* particle camera ROSINA (Fig. 5.3.5) is a highly flexible and modular system. It features a 29 megapixel camera with dual GigE interface and a modular optical concept to be able to cover a wide range of magnifications and field of views (FoVs). A PC104 computer stack on the frame is used to run the system. Remote access to this computer stack via a telemetry unit and the standard CTD wire (11 mm coax) enables the user to control the system, make modifications of settings and view images during the deployment.

The components of the In-Situ Optical Device Unit (camera, PC104 stack, telemetry device part, lithium-ion battery, Seabird™ SBE19 CTD, backlight source and reflective light source) are mounted on a stainless steel frame (Fig. 5.3.5, left image). The Deck System consists of the telemetry deck part (Fig. 5.3.5, top part in right image) and the user interface unit (Fig. 5.3.5, bottom part in right image), which consists of a KVM console, one Windows and one Linux computer, a NAS storage and an Ethernet switch. All these parts are mounted in two plywood boxes. A functional overview of the system can be seen in Figure 5.3.6.


**Fig. 5.3.5** The ROSINA system consists of two parts, the In-Situ Optical Device (left) and the Deck System (right).

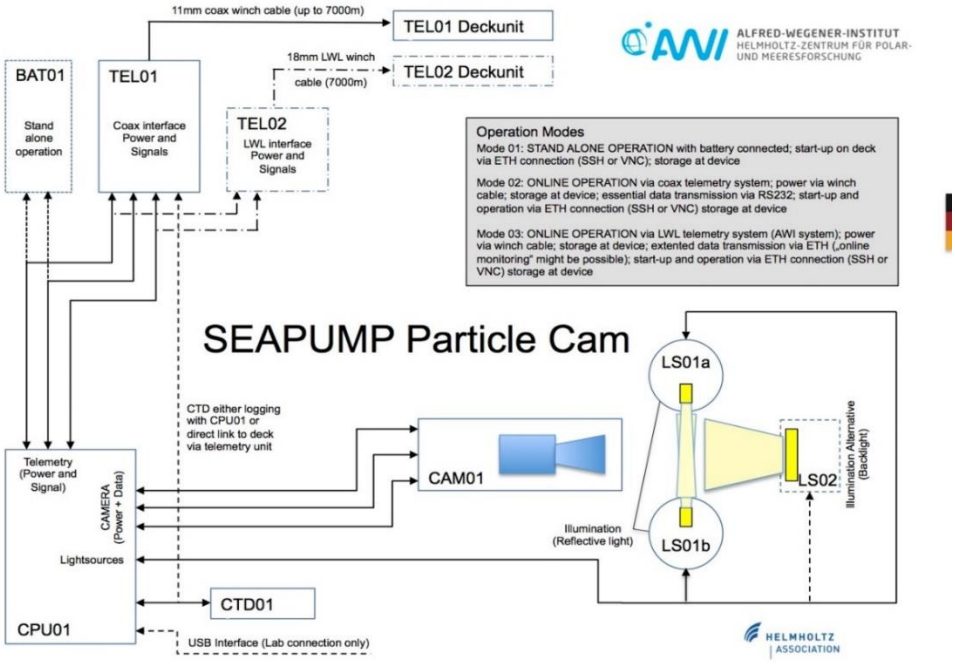


**Fig. 5.3.6** Functional overview of the ROSINA system.

The system is able to generate up to four images per second with a resolution of 6576 x 4384 pixels. All camera features are fully controllable by the user due to a custom made GUI (based on C++ and Qt). Furthermore there is the possibility of getting shadow images with the backlight source (white background) and reflective light images (black background).

The aim of ROSINA deployments on this cruise was to get the system running and test different optical configurations and modes in real application. It was the first time operated via a 11 mm CTD wire (in this case approx. 6000 m in length) and the maximum possible communication speed is 1 MB with that cable length, which is fine for controlling the system remotely. Nevertheless, powering the system via telemetry unit was not possible over that cable length.

During the cruise we made six deployments (Table 5.3.3) with different optical configurations. We successfully tested the backlight and the reflective light sources and two different lens configurations with an object field of view of approx. 62 x 42 mm and 26 x 18 mm. Due to the early stage of the development, image processing scripts are not implemented and finished yet. As a proof of operation of the system some example images taken during the deployments should give an impression of the power of the system (Fig. 5.3.7).

**Table 5.3.3** List of ROSINA stations.

| Profile No. | Station No | Date | Start Time | Latitude | Longitude | Water depth (m) | Profile depth (m) |
|---|---|---|---|---|---|---|---|
| 1 | MSM77_33-2 | 25.09.2018 | 16:56:00 | 79°42.086'N | 10°00.097'E | 164 | 100 |
| 2 | MSM77_35-1 | 27.09.2018 | 08:43:00 | 79°04.006'N | 04°10.066'E | 2415 | 500 |
| 3 | MSM77_46-3 | 01.10.2018 | 17:44:47 | 78°32.948'N | 01°50.205'W | 2711 | 500 |
| 4 | MSM77_53-2 | 04.10.2018 | 10:39:30 | 79°44.186'N | 04°29.118'E | 2609 | 200 |
| 5 | MSM77_57-1 | 06.10.2018 | 04:13:20 | 79°01.312'N | 10°50.962'E | 321 | 50 |
| 6 | MSM77_57-2 | 06.10.2018 | 05:19:45 | 79°01.312'N | 10°50.962'E | 321 | 50 |

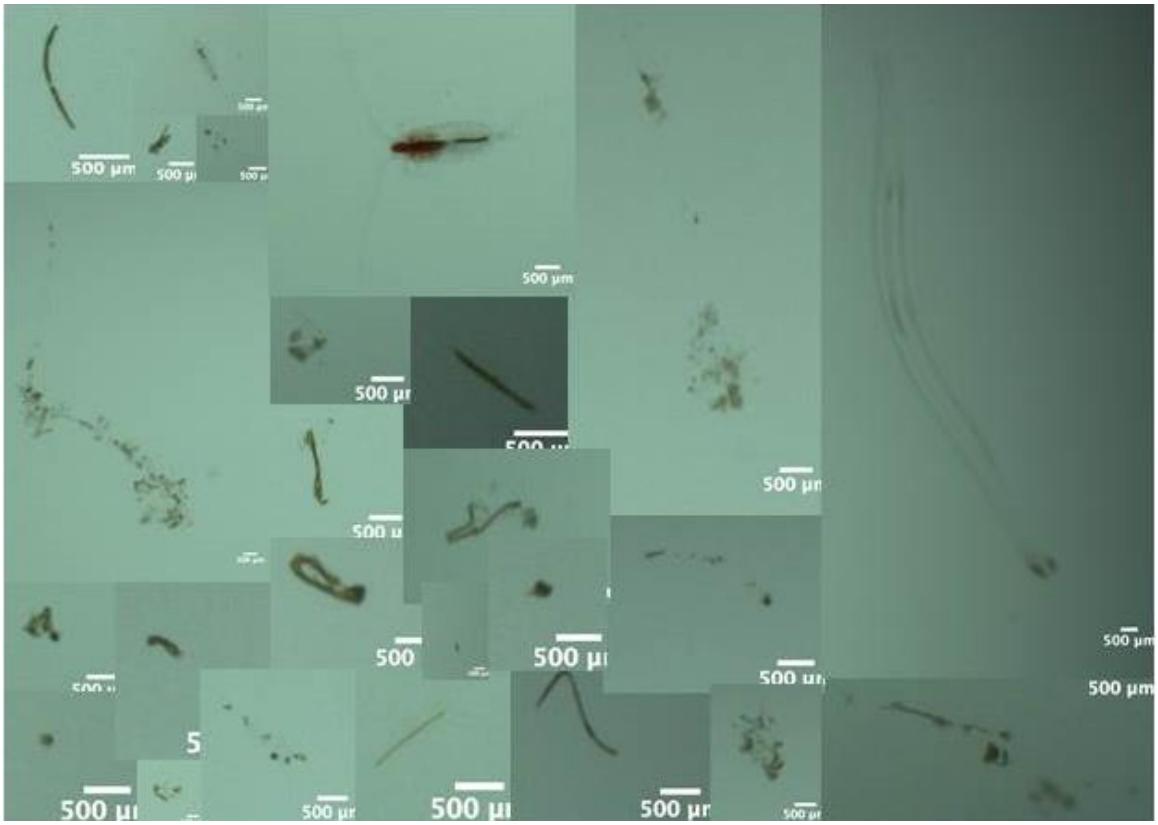


**Fig. 5.3.7** Example images of ROSINA during deployment #3 with backlight. The object pixel size is 9.4 µm and the detected volume of one image (6576 x 4384 pixels) is approx. 125 ml.

- *Marine Snow Catcher*

We deployed 13 Marine Snow Catchers (MSC) to collected *in situ* formed marine snow. The MSCs consisted of a 100 L cylindrical water sampler with a particle collection tray at the bottom (Fig. 5.3.8). They were deployed with a winch to the target depth and closed via a release mechanism that was activated with a drop weight (Table 5.3.4). The closed MSCs were placed on deck for a few hours to allow the collected particles to sink to the collection tray at the lower part of the instrument. We gently drained the water from the 100 L cylinder and removed the collection tray, which now contained the settling particles.


**Fig. 5.3.8** The Marine Snow Catcher (MSC) was deployed via the ship's winch system and lowered to a specific water depth, where after it was closed by a messenger weight and releaser. After recovery the MSC was positioned up-right on deck to allow the particles to settle to the bottom part of the MSC.

**Table 5.3.4** Deployments of the marine snow catcher with information about station name, MSC number, date of deployment, time for deployment, latitude, longitude, and deployment depth.

| Station name | MSC # | Date | Time (UTC) | Latitude | Longitude | Depth (m) |
|---|---|---|---|---|---|---|
| MSM77_3-3 | MSC 1 | 17.09.2018 | 00:22 | 78°36.99'N | 05°04.08'E | 40 |
| MSM77_4-4 | MSC 2 | 17.09.2018 | 18:09 | 79°03.55'N | 04°12.01'E | 40 |
| MSM77_13-2 | MSC 3 | 20.09.2018 | 16:40 | 79°08.00'N | 06°05.54'E | 45 |
| MSM77_17-2 | MSC 4 | 21.09.2018 | 23:04 | 79°01.80'N | 06°59.89'E | 40 |
| MSM77_17-3 | MSC 5 | 21.09.2018 | 23:16 | 79°01.80'N | 06°59.89'E | 40 |
| MSM77_21-2 | MSC 6 | 22.09.2018 | 19:36 | 79°00.22'N | 08°16.83'E | 60 |
| MSM77_22-2 | MSC 7 | 23.09.2018 | 00:48 | 78°58.81'N | 09°30.84'E | 15 |
| MSM77_43-1 | MSC 8 | 30.09.2018 | 21:48 | 79°08.02'N | 02°50.60'E | 40 |
| MSM77_43-2 | MSC 9 | 30.09.2018 | 22:02 | 79°08.02'N | 02°50.60'E | 40 |
| MSM77_52-2 | MSC 10 | 03.10.2018 | 23:39 | 79°56.29'N | 03°11.76'E | 25 |
| MSM77_52-3 | MSC 11 | 03.10.2018 | 23:55 | 79°56.29'N | 03°11.76'E | 25 |
| MSM77_54-2 | MSC 12 | 04.10.2018 | 20:01 | 79°36.23'N | 05°10.36'E | 20 |
| MSM77_56-2 | MSC 13 | 05.10.2018 | 18:06 | 79°03.62'N | 04°07.62'E | 20 |

We used the collected aggregates to determine their size-specific sinking velocities, microscopic observations of the aggregate composition, and measurements of respiration of the aggregate attached microbes. The aggregate size, sinking velocities, and microbial respiration were measured in a vertical flow chamber. The vertical flow system was filled with GF/F filtered surface water from each station at *in situ* temperature. Individual aggregates were placed in the flow chamber and the upward flow was increased until the aggregate remained suspended in the flow chamber. The sinking velocity of each aggregate was calculated from the flow rate divided by the cross-sectional area of the flow chamber. Triplicate measurements of sinking velocity were made for each pellet. The length of all three pellet axes (length, width, and height direction) was measured while in the flow system using a horizontal dissection microscope with a calibrated ocular lens. The aggregate volume was calculated by assuming an ellipsoid shape. For comparison between different aggregate shapes, we calculated the equivalent spherical diameter (ESD) of each aggregate.

Oxygen gradients through the aggregate-water interface were measured using a Clark-type oxygen microelectrode mounted in a micromanipulator and calibrated at air-saturation and at anoxic conditions. The electrode current was measured with a Unisense™ Multimeter and the computer program SensorTrace Pro (Unisense™). The tip diameter of the microsensor was 12 µm and the 90% response time of the electrode was <1 sec with a stirring sensitivity of <0.3%. The pellets were suspended by an upward-directed flow that balanced their sinking velocities during the measurements. The oxygen gradients were measured in steps of 25 µm through the boundary layer between the pellet surface and the ambient water. The oxygen gradients were measured on the downstream side of the

pellets, which has been shown to be representative of the whole boundary layer. We only measured during steady state in GF/F filtered surface water at *in situ* temperature. After determination of size, settling velocity, and microbial respiration, the aggregates were microscopically imaged and frozen for biogeochemical analyses in the home laboratory.

## 5.4 Operating an Autonomous Underwater Vehicle (AUV) to investigate Frontal Systems in Surface Waters and conduct extensive Mapping at the Deep Seafloor

(T. Wulff, M. Busack, J. Hagemann, S. Lehmenhecker)

The RV MARIA S. MERIAN expedition MSM77 was used to conduct dives with the Autonomous Underwater Vehicle (AUV) PAUL operated by the Deep-Sea Research Group at the Alfred Wegener Institute (Fig. 5.4.1). PAUL is a 4.5 m long torpedo-shaped vehicle which is depth rated to 3000 m water depth. At a speed of about 5-6 km per hour, comparable to a fast walking pedestrian, it can cover distances of 70 km. PAUL is propelled by a single gimbal ducted thruster at its stern, which can be moved in every direction and thus provides thrust and attitude control. The vehicle operates with no physical connection to a support vessel and without direct human surveillance. Thus, it offers an extremely efficient way to cover (ship)time-consuming tasks. With respect to this particular characteristics of the vehicle, two objectives were pursued within the framework of MSM77:

1. High resolution water column studies to investigate the interaction between ice, ocean and atmosphere and to reveal the ecological impact of this interaction. The applied configuration of the vehicle is named “BGC configuration”.
2. Conduct benthic operations and map the seafloor with a newly integrated sidescan sonar. These operations entail deep dives. The applied configuration of the vehicle is called “benthic configuration”.

It is especially the second objective that sets MSM77 apart from other cruises. Whereas water column studies have been accomplished in previous cruises, for example in 2013 during MSM29, and proofed to be very complex in execution, mapping missions are a new field for AWI’s AUV team. MSM77 thus was the first cruise the vehicle was operated with two completely different payload sections in completely different mission settings. With this regard, MSM77 marks the successful end of a process launched in early 2017 to improve the vehicle and its surrounding infrastructure and eventually transform it into a truly versatile platform.

**Fig. 5.4.1** PAUL in its BGC configuration prior to trimming off the coast of Svalbard (© M. Busack).

## Technical description

- *Payload set-up of the BGC configuration*

In the BGC configuration the vehicle carries the following instruments:

- Conductivity sensor
- Temperature sensor
- Pressure sensor

} all in one instrument: CTD probe

- Photosynthetically Active Radiation sensor (PAR)
- Dissolved Oxygen sensor (DO)
- 4 x Microstructure probes velocity shear
- 3 x Microstructure probes temperature
- Fluorometer for Coloured Dissolved Organic Matter (CDOM)
- Fluorometer for Chlorophyll *a* (Chl. *a*)
- Nitrate sensor

In addition to that, PAUL is equipped with a water sample collector, which can collect up to 22 samples with an overall volume of 4.8 L of sample material (Fig. 5.4.2).

- *Payload set-up of the benthic configuration*

In the benthic configuration the vehicle carries a Sidescan sonar with the transducers being attached to the outside of the payload section (Fig. 5.4.2). The sonar has two operational frequencies of 600 and 1200 kHz. A higher frequency entails a higher resolution, yet the vehicle needs to fly over the seafloor at a lower altitude (600 kHz: 13-26 m, 1200 kHz: 4.5-9 m).

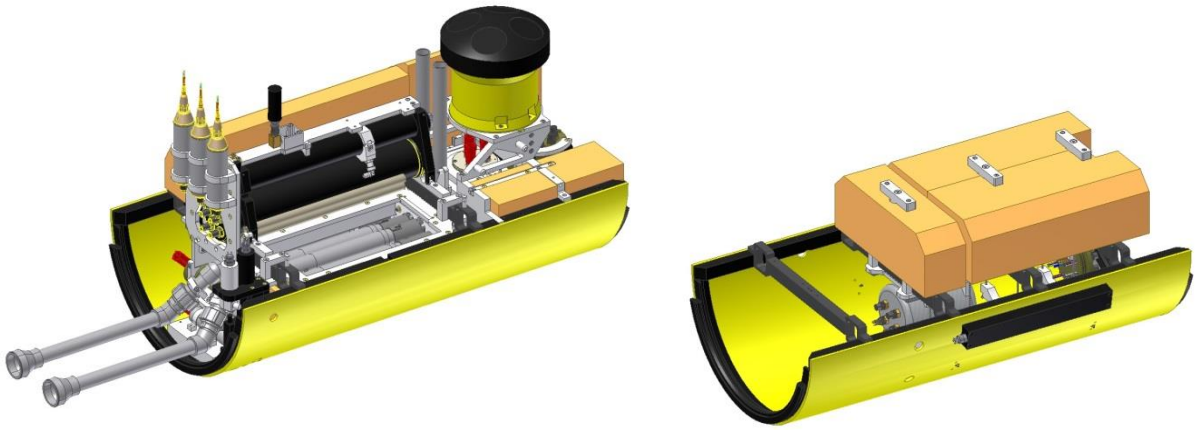

**Fig. 5.4.2** BGC payload (left) and benthic payload (right) of the Autonomous Underwater Vehicle PAUL.

## Dives

In total, the vehicle was deployed six times and five dives were completed successfully. Table 5.4.1 summarizes selected dive data.

**Table 5.4.1** Overview on AUV deployments.

| No / Dive ID Date | Deployment Position | Duration [hh:mm] | Distance [km] | Config. | Max. Depth | Samples |
|---|---|---|---|---|---|---|
| 1 / 048 18.09.2018 | 79°03.215‘N / 03°35.626‘E | 02:30 | 9.4 | BGC | 101 | 15 |
| 2 / 049 20.09.2018 | -- | -- | -- | Benthic | -- | -- |
| 3 / 050 21.09.2018 | 78°39.145‘N / 09°24.814‘E | 04:45 | 21.1 | Benthic | 215 | -- |
| 4 / 051 22.09.2018 | 78°59.960‘N / 08°41.840‘E | 01:23 | 6.0 | Benthic | 227 | -- |
| 5 / 052 29.09.2018 | 79°06.596‘N / 04°52.832‘E | 02:20 | 10.9 | Benthic | 1514 | -- |
| 6 / 053 06.10.2018 | 79°01.053‘N / 11°30.191‘E | 03:27 | 19.4 | Benthic | 345 | -- |

- *Dive 1 (Dive ID: 048)*

The first dive of MSM77 took place on September 18th and had a technical background. As the vehicle was transported by trailer, basic vehicle functions needed to be checked by executing a number of short dives with increasing complexity. As the dive behaviour of the vehicle is considered to be more critical with the BGC payload attached, the dive was conducted in the vehicle's BGC configuration.

In the beginning, the trim turned out to be insufficient to make the vehicle submerge and it needed to be recovered to add ballast (Fig. 5.4.3). Eventually, five missions with a maximum depth of 100 m were completed successfully. Most critical tests could be accomplished and 15 water samples were collected and processed. The samples were to provide a baseline calibration of the vehicle's Chl. *a* fluorometer and nitrate sensor.

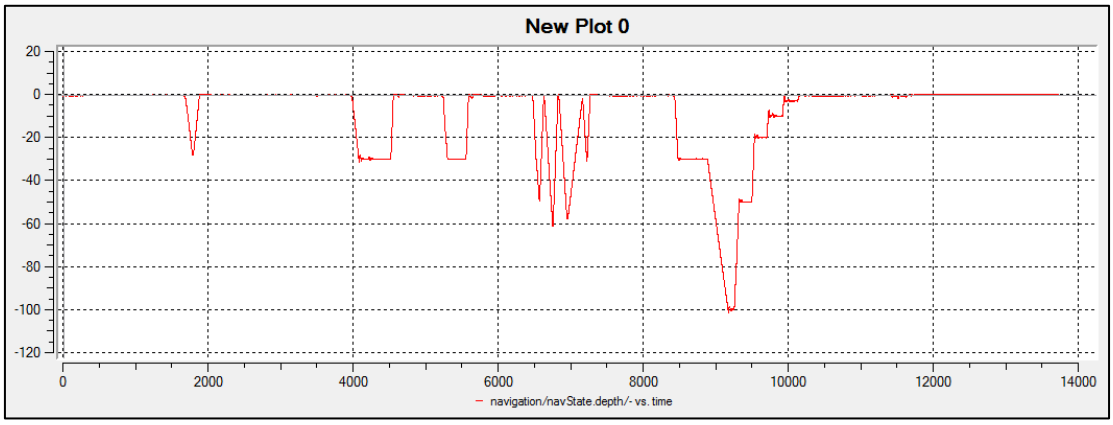


**Fig. 5.4.3** Profiles of the individual missions of Dive 1 (Depth vs. mission time).

- *Dive 2 (Dive ID: 049)*

The second dive of the vehicle, which was intended to be the first in the Benthic configuration, had to be cancelled due to an issue with the navigation system. The vehicle's Doppler Velocity Log (DVL), which is a crucial part of the navigation system, failed running due to a network error. The issue could be fixed the following day.

- *Dive 3 (Dive ID: 050)*

After the DVL failed running in the previous dive, the third dive of the cruise was the first test with the vehicle´s benthic configuration. The area of interest was the gas hydrate stability zone (GHSZ) off the coast of Svalbard where the vehicle had already accomplished a dive in 2012 (dive ID: 022). Here, in roughly 250 m water depth, melting gas hydrates release large amounts of methane into the ocean.

To identify locations with active gas emissions, the area was surveyed using the ship's multi-beam sonar with the objective to find gas flares. The vehicle was deployed, although no gas flares had been observed.

The dive consisted of two phases. In the first phase, vehicle navigation and especially its autonomous approach to the seafloor were tested to make sure that the sonar does not interfere with the navigation system. The vehicle performed a spiral descent and autonomously detected the altitude threshold of 50 m above the seafloor, which successfully terminated the descent and eventually triggered the ascent behaviour to return to the surface.

In the second phase, the vehicle was to cover a survey rectangle over locations where gas was emitted in 2012. However, due to a programming error, the vehicle did not reach its intended depth and sonar data were collected in the open water column – without receiving a useful echo.

- *Dive 4 (Dive ID: 051)*

The fourth dive of the vehicle took place in the eastern Fram Strait at the continental shelf. The depth of the area was roughly 270 m. As the reason for the error of the previous dive, where the vehicle did not reach its mission depth, was still unclear at this time, the dive was again divided into two phases. In the first phase, the vehicle performed an autonomous approach to the seafloor and completed a short survey rectangle at a safe altitude of 100 m above ground (Fig. 5.4.5). After this initial test, the vehicle descended again in a spiral and autonomously inserted into a survey rectangle with four legs covering an area of 450 x 150 m at an altitude of 20 m above the seafloor. With the 600 kHz channel of the sidescan sonar being activated, this mission marks the first successful benthic operation of the vehicle.

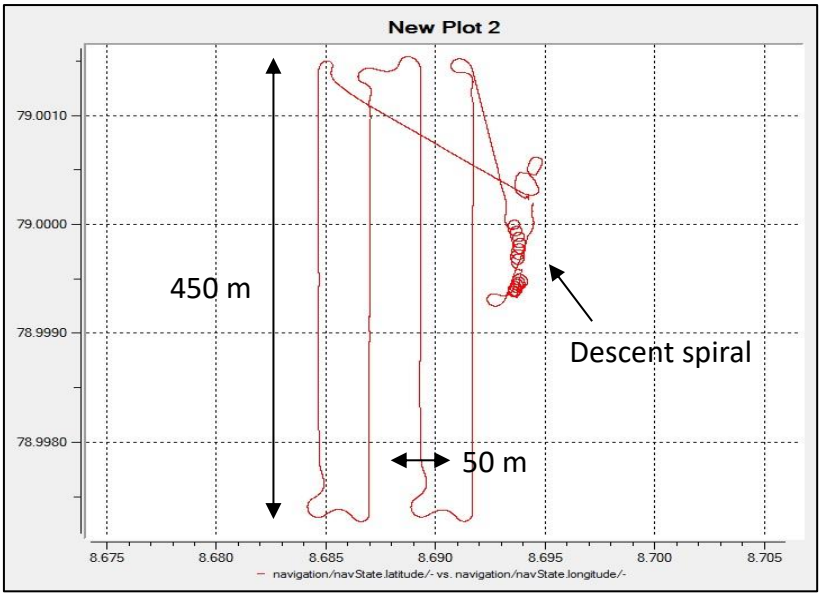


**Fig. 5.4.5** Dive track of the second phase of the fourth dive – the first successful benthic mission.

- *Dive 5 (Dive ID: 052)*

Sonar images of the previous dive showed the seafloor to be relatively undefined – providing almost no visible "target" for a sonar system. Thus, during the fifth dive of the vehicle, NOMAD, a benthic crawler which was standing on the seafloor at HG-III, served as an easily recognizable target with known dimensions.

As NOMAD stood at 1500 m water depth, it was calculated the vehicle would need about 25-30 minutes for the descent. During this time, the vehicle is solely dependent on its INS which would perform a dead reckoning until the DVL detects the seafloor and uses it as a fixed reference. To minimize the drift induced error, the descent behaviour was kept as easy as possible. Thus, unlike the previous dives, when the vehicle descended in a complex spiral, it now took a straight path at a pitch angle of -30° to reach the intended mission altitude (20 m above seafloor). Additionally, the ship's ADCP was used to determine velocity and direction of the water currents and PAUL's descent path was orientated so that it would constantly drive against the current. Within 20 minutes, the vehicle covered two 500 m long survey legs at 20 m altitude. It exactly crossed the location of NOMAD, which we were later able to identify in the sonar data (Fig. 5.4.6).

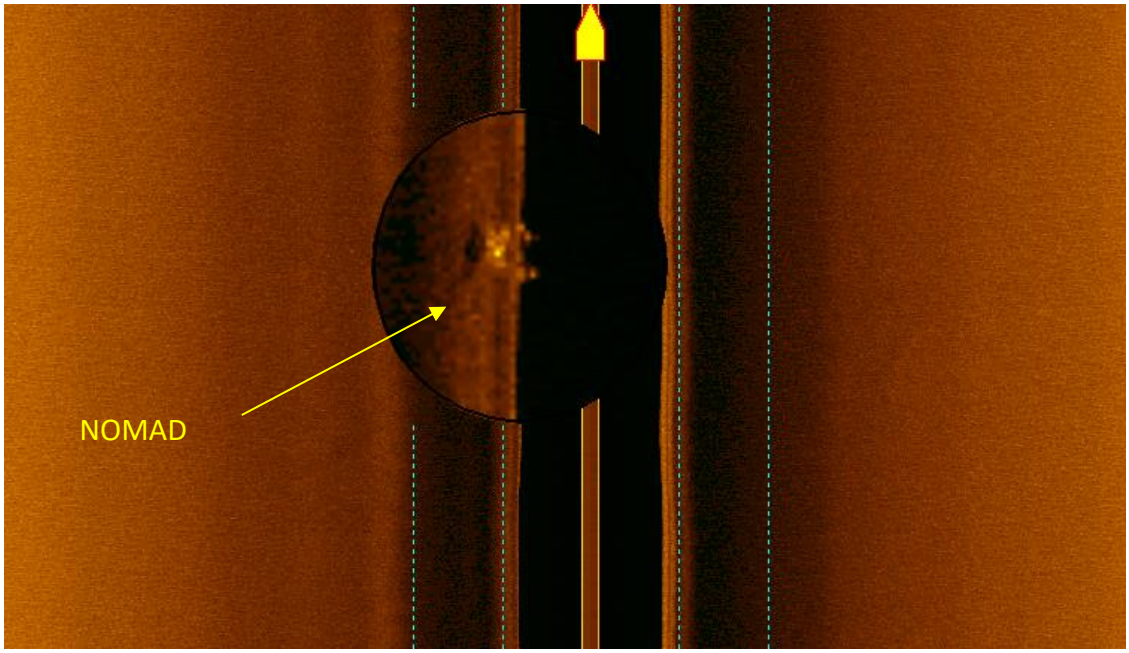


**Fig. 5.4.6** NOMAD standing in about 1500 m water depth at HG-III as it was visible in the 600 kHz channel of PAUL's sidescan sonar.

- *Dive 6 (Dive ID: 053)*

The vehicle's last dive took place inside the Kongsfjord as the wave height at the original deployment position off the coast of Svalbard was too high to successfully deploy the vehicle. Inside the fjord, the seafloor was investigated using the ship's multi-beam sonar and an area with promising topography was identified as a target for the vehicle's sidescan sonar. The area featured steep subsea slopes (~70 m altitude difference on 600 m horizontal distance) and the depth was about 300 m. After a first initial dive to check critical vehicle functions and underwater tracking, the vehicle performed three identical rectangular surveys of the same area. Each of the surveys consisted of five 800 m long survey legs with a strict longitudinal orientation (Fig. 5.4.7). The spatial distance between the legs was 50 m, thus the investigated area was 800 x 200 m in size. Although the survey rectangles were identical in shape and location, the surveys were performed with decreasing altitude (20 m, 15 m, 10 m) to check the sonar's resolution. For the first time in a mission, both channels of the sidescan sonar (600 + 1200 kHz) were activated simultaneously during this dive.

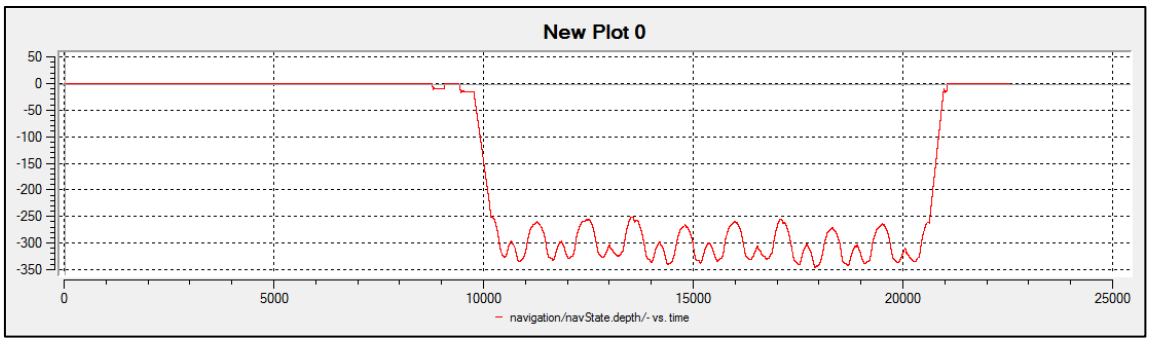


**Fig. 5.4.7** Dive profile of PAUL's sixth dive. Note the strong oscillations which represent steep slopes.

- *CTD section (03.-04.10.2018)*

Following the original cruise planning, the vehicle and its BGC payload were supposed to be operated at frontal systems (boundary regions between different water masses) to reveal the interaction between physics and ecology at these very particular features. We anticipated to encounter frontal systems in the second half of the cruise when the ship would operate close to the ice in the central Fram Strait. However, due to weather constraints, AUV operations were cancelled when the ship reached an area where frontal systems were present. To at least partially compensate for that, AUV measurements were replaced by a high resolution, shallow CTD section (Table 5.4.2). The target area of this section was an ice tongue which could be identified in satellite images days before. The section followed an orientation of 33° to provide a cross-section through the ice tongue and the associated water masses (Fig. 5.4.8).

**Table 5.4.2** Station details of the CTD transect to study a frontal system in the vicinity of an ice tongue ("x" indicates that sample was taken, whereas "o" indicates that it was omitted).

| Station MSM77_ | Time Start | Position | | Max. Depth | Sample, Depth [m] | | | | Nutrients | Chl. a | Plankton |
|---|---|---|---|---|---|---|---|---|---|---|---|
| | UTC | Lat | Lon | m | 1 | 2 | 3 (Chl max) | 4 | | | |
| 49-1 | 14:57 | 79°19.360'N | 00°48.090'E | 100 | 100 | 30 | 15 | 5 | x | o | x |
| 49-2 | 16:13 | 79°22.125'N | 00°39.209'E | 50 | 50 | 30 | 15 | 5 | x | o | o |
| 49-3 | 17:18 | 79°24.994'N | 00°30.032'E | 50 | 50 | 30 | 15 | 5 | x | o | x |
| 49-4 | 17:46 | 79°25.605'N | 00°32.312'E | 100 | 100 | 30 | 15 | 5 | x | o | o |
| 49-5 | 18:25 | 79°26.270'N | 00°34.307'E | 50 | 50 | 30 | 15 | 5 | x | o | o |
| 49-6 | 19:08 | 79°26.892'N | 00°37.211'E | 50 | 50 | 30 | 15 | 5 | x | x | o |
| 49-7 | 19:42 | 79°27.519'N | 00°39.212'E | 50 | 50 | 30 | 15 | 5 | x | o | o |
| 49-8 | 20:15 | 79°28.209'N | 00°41.492'E | 70 | 70 | 30 | 15 | 5 | x | x | x |
| 49-9 | 20:48 | 79°28.866'N | 00°44.251'E | 70 | 70 | 30 | 15 | 5 | x | o | o |
| 49-10 | 21:18 | 79°29.601'N | 00°46.519'E | 70 | 70 | 30 | 15 | 5 | x | o | o |
| 49-11 | 21:54 | 79°30.225'N | 00°48.860'E | 70 | 70 | 30 | 15 | 5 | x | x | x |
| 49-12 | 22:36 | 79°30.893'N | 00°50.860'E | 70 | 70 | 30 | 15 | 5 | x | o | o |
| 49-13 | 23:25 | 79°31.575'N | 00°53.339'E | 70 | 70 | 30 | 15 | 5 | x | x | x |
| 49-14 | 00:07 | 79°32.308'N | 00°55.951'E | 70 | 70 | 30 | 15 | 5 | x | o | o |
| 49-15 | 00:45 | 79°32.976'N | 00°58.272'E | 70 | 70 | 30 | 15 | 5 | x | o | o |
| 49-16 | 01:22 | 79°33.617'N | 01°00.576'E | 70 | 70 | 30 | 15 | 5 | x | x | x |
| 49-17 | 01:57 | 79°34.273'N | 01°03.126'E | 70 | 70 | 30 | 15 | 5 | x | o | o |
| 49-18 | 02:40 | 79°34.932'N | 01°05.726'E | 70 | 70 | 30 | 15 | 5 | x | o | o |
| 49-19 | 03:46 | 79°35.460'N | 01°08.397'E | 70 | 70 | 30 | 15 | 5 | x | x | x |
| 49-20 | 04:26 | 79°36.135'N | 01°10.308'E | 70 | 70 | 30 | 15 | 5 | x | o | o |
| 49-21 | 05:05 | 79°36.889'N | 01°12.304'E | 70 | 70 | 30 | 15 | 5 | x | o | o |
| 49-22 | 05:42 | 79°37.513'N | 01°15.020'E | 70 | 70 | 30 | 15 | 5 | x | x | x |
| 49-23 | 06:16 | 79°38.256'N | 01°17.561'E | 70 | 70 | 30 | 15 | 5 | x | o | o |
| 49-24 | 07:00 | 79°38.936'N | 01°19.957'E | 70 | 70 | 30 | 15 | 5 | x | o | o |
| 49-25 | 07:36 | 79°39.620'N | 01°22.031'E | 70 | 70 | 30 | 15 | 5 | x | x | x |
| 49-26 | 08:29 | 79°40.214'N | 01°24.592'E | 70 | 70 | 30 | 15 | 5 | x | o | o |
| 49-27 | 09:12 | 79°40.896'N | 01°27.153'E | 70 | 70 | 30 | 15 | 5 | x | o | o |
| 49-28 | 09:49 | 79°41.545'N | 01°29.410'E | 70 | 70 | 30 | 15 | 5 | x | x | x |
| 49-29 | 10:28 | 79°42.214'N | 01°31.866'E | 70 | 70 | 30 | 15 | 5 | x | o | o |
| 49-30 | 11:08 | 79°42.877'N | 01°34.395'E | 70 | 70 | 30 | 21 | 5 | x | o | x |
| 49-31 | 11:49 | 79°43.573'N | 01°36.751'E | 70 | 70 | 37 | 22 | 5 | x | x | x |
| 49-32 | 12:25 | 79°44.238'N | 01°39.033'E | 70 | 70 | 35 | 15 | 5 | x | o | x |
| 49-33 | 13:00 | 79°44.992'N | 01°41.520'E | 70 | 70 | 48 | 12 | 5 | x | x | x |

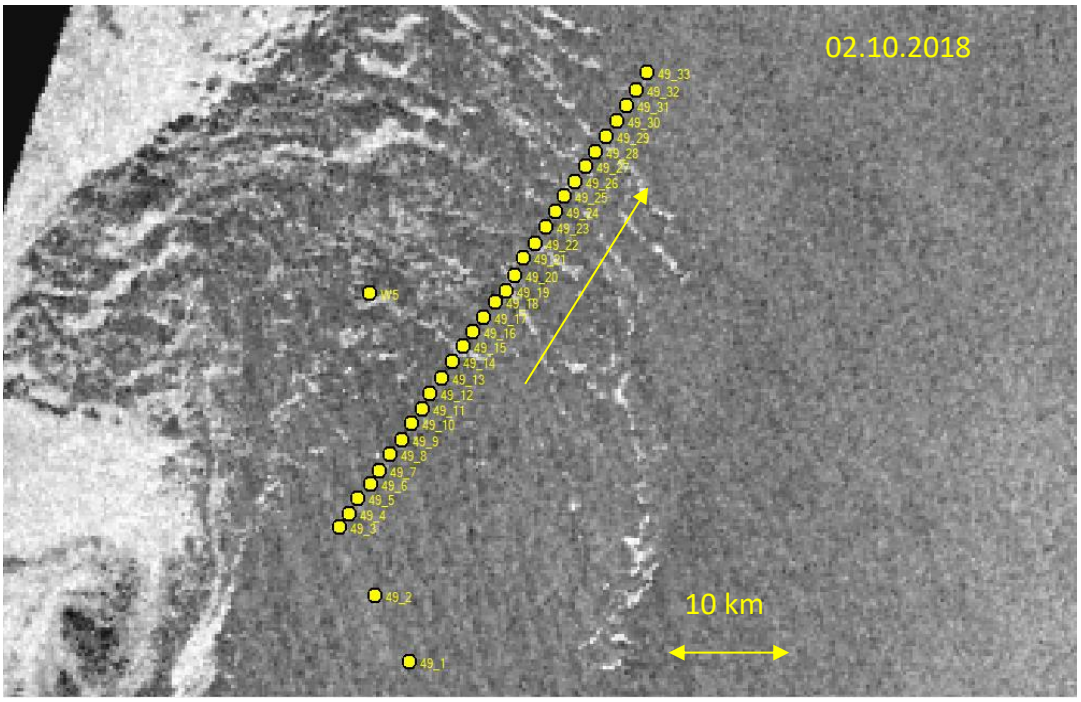


**Fig. 5.4.8** Positions of the CTD casts for the high resolution section.

The standard depth of the individual casts was 70 m (in some cases 50 m or 100 m) and the horizontal distance between the casts was 1.5 km. By default, the ship's CTD/Rosette Water Sampler is equipped with sensors for conductivity, temperature, pressure, dissolved oxygen and a Chl. *a* fluorometer. To gather consecutive nitrate data, the AUV's nitrate sensor was taken from the BGC payload and integrated into the CTD system.

In addition to that, water samples were taken from four distinct water depths using the Rosette Water Sampler's Niskin bottles. At every cast, a subsample of 8 ml was preserved to be analysed for macronutrients (Nitrate, Nitrite, Phosphate, Ammonium, Silicate). At roughly every third cast, subsamples were taken from the chlorophyll maximum for filtration (to measure Chl. *a* content) and to determine phytoplankton species. To further investigate the physical conditions in the investigated area, the AUV's Acoustic Doppler Current Profiler (ADCP) was lowered from the ship's moon-pool. In contrast to the ship's ADCP, which operates at 75 kHz, the AUV's ADCP operates at 300 kHz, which provides a higher resolution and a sufficient range (~80 m).

Preliminary results of the experiment are shown in Figure 5.4.9. A low saline and cold (data not shown) waterbody, presumably of polar origin, overlaps a waterbody of higher salinity. Further analysis will include wind speed and direction to explain the evolution of the observed structures. Eventually, these physical data are supposed to be put into relation to the ecological data such as Chl. *a* concentration and plankton species composition.

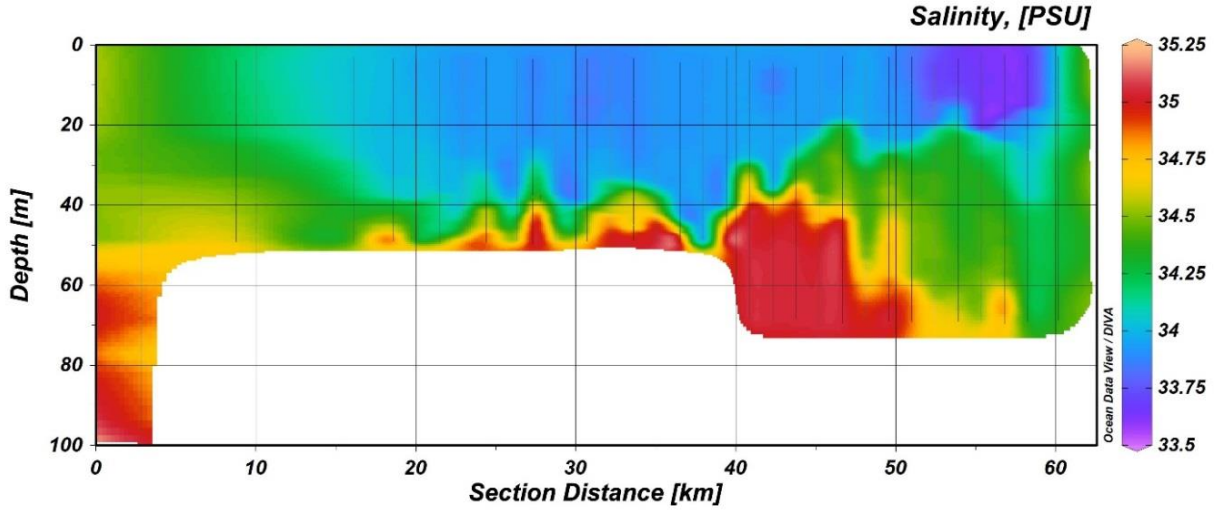


**Fig. 5.4.9** Salinity data along the CTD transect sampled to study a frontal system in partially ice-covered areas off NE Greenland.

## 5.5 Oxygen Consumption Rates to access Benthic Carbon Mineralization

(F. Wenzhöfer, M. Hofbauer, A. Nordhausen, A. Sonnek)

Benthic organic matter remineralization rates were assessed based on oxygen uptake rates measured *in situ*. Micro-scale distributions of oxygen at the sediment water interface and within the sediments were studied in order to assess diffusive oxygen uptake rates (DOU). In order to quantify total oxygen consumption rates (TOU, i.e. DOU plus fauna-mediated oxygen uptake) sediments were enclosed and oxygen decrease in the overlying water monitored. For short-term investigations a Flux-Lander was used while two benthic crawler systems were used to study the seasonal variation.

### Flux-Lander

An autonomous benthic lander system was used to study benthic oxygen uptake and fluxes of other solutes at the sediment water interface. The lander was equipped with three benthic chambers and a 2-axis re-locatable microprofiler.

- *Benthic chambers*

After arrival at the seafloor the benthic chambers enclose a 0.04 $m^2$ large sediment patch together with an approx. 0.15 m high layer of overlying water. During the respective deployments the overlying water was kept mixed by gentle stirring and changes in oxygen concentrations were monitored by means of optical oxygen sensors attached to the chamber lid. At pre-programmed times a total of

seven samples per chamber were taken from the overlying water. Total fluxes of oxygen (TOU) across the sediment-water interface are calculated from the change in concentration per time (as determined from optode recordings or discrete measurements obtained from samples) times overlying water column height.

- *Microprofiler*

The fine-scale distribution of dissolved oxygen across the sediment-water interface and within pore waters was determined by means of Clark-type oxygen micro-electrodes that were incrementally inserted into the sediment. The individual sensors were custom-made from glass with typical tip-diameters in the range of some tens of micrometres. Up to nine oxygen electrodes were attached to a 150 mm diameter titanium housing that contained electronics for signal amplification and processing. In addition to the linear drive responsible for vertical profiling a second, horizontally-oriented drive allowed for lateral relocation of the electronic housing and sensors between profiler runs to make sure that replicate profiles were measured at distinct sediment spots. Diffusive oxygen uptake is calculated from the change in oxygen concentration across the diffusive boundary layer (DBL) or the uppermost sediment layer times the diffusion coefficient d (T, S) or based on the derivative of the entire profile.

**Benthic crawler**

The fully autonomous benthic crawler TRAMPER is capable to record sediment oxygen distributions over a full annual cycle with translocation between consecutive measurements. The new generation of optode-based oxygen monitoring system mounted on the crawler will help to establish high-temporal resolution benthic flux measurements in order to determine seasonal variations in organic matter turnover and benthic community respiration activity.

During its mission the crawler, equipped with a multi-optode profiler, was pre-programmed to perform >52 sets of vertical concentration profiles across the sediment-water interface (one set each week) along a ~1 km transect.

The second benthic crawler NOMAD, which will additionally study seasonal variations in biogeochemical processes at the seafloor, is an extended version of TRAMPER. Besides measuring oxygen consumption rates with microprofiles and two benthic chambers, NOMAD is able to take images of the seafloor topography and spatial distribution of the settling labile organic matter.

Both crawler systems allow now to investigate the deep seafloor in remote areas and over longer time periods, which was previously not possible.

**Deployments and data obtained**

The Flux-Lander was deployed three times at HAUSGARTEN time series stations S3, FL-2 and HG-IX. All in all, deployments during MSM77 resulted only in one successful measurement at S3. At the shallow site FL-2 (290 m water depth) the seafloor was densely covered with stones preventing the chambers and microsensors to penetrate into the sediment. At the deep sites HG-IX (5500 m water depth) the lander got lost as it did not return after sending the release command.

The crawler TRAMPER was successfully recovered after its one-year mission at HG-IV (Fig. 5.5.1). When recovered, TRAMPER had moved for a distance of ca 800 m and performed 54 measurement cycles. The first investigation of the data showed that TRAMPER performed 48 successful measurements which will help to improve our knowledge about the seasonal variations of the oxygen distribution in the sediments. The retrieved oxygen profiles will be used to calculate weekly benthic oxygen consumption rates which can then be converted to carbon equivalents. This allows determining the seasonal variations in organic matter mineralization.

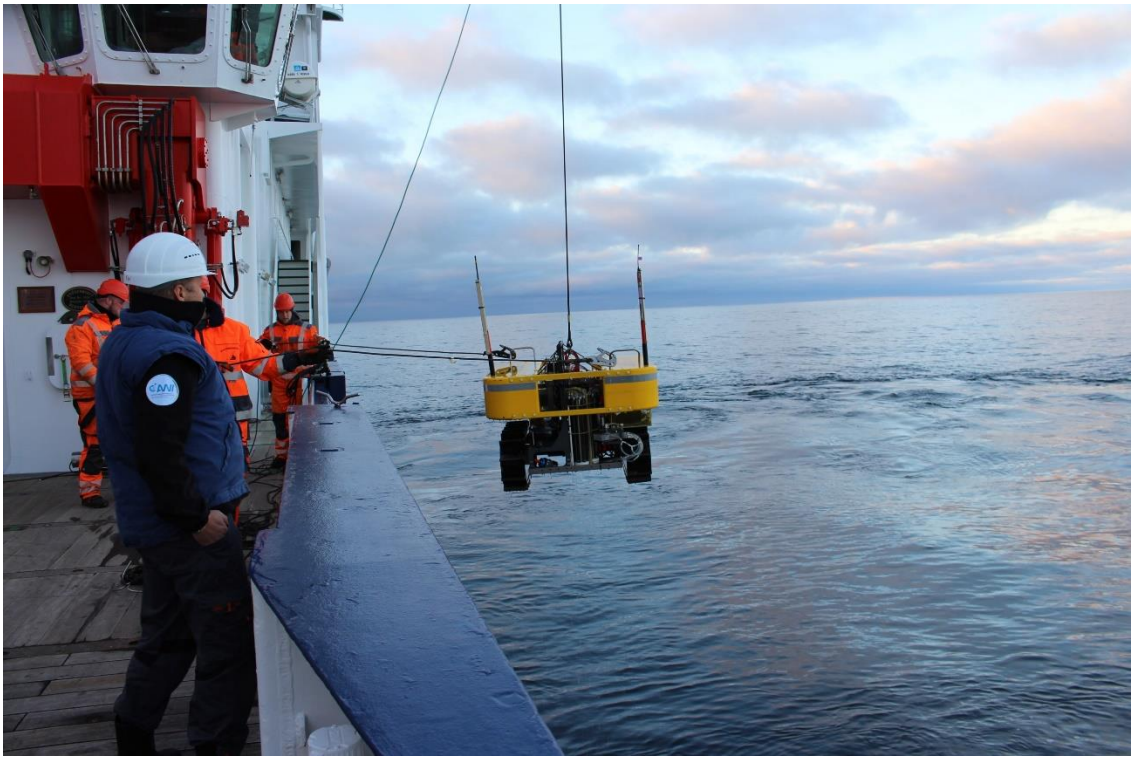

**Fig. 5.5.1** TRAMPER recovery after its one-year mission at the seafloor.

After recovery, TRAMPER was renewed (exchange of sensors and batteries) and deployed again for its third 12-month mission at the deep seafloor. We will recovery TRAMPER next year during RV POLARSTERN cruise PS121. The second crawler NOMAD was tested at HG-II (Fig. 5.5.2). The deployment showed that the system generally works, but due to some mechanical problems the crawler did not move as programmed. Additionally, the ballast release system did not work properly and thus the crawler had to be recovered using hooks mounted on the towed camera system OFOS (Ocean Floor Observation System) (Fig. 5.5.3).

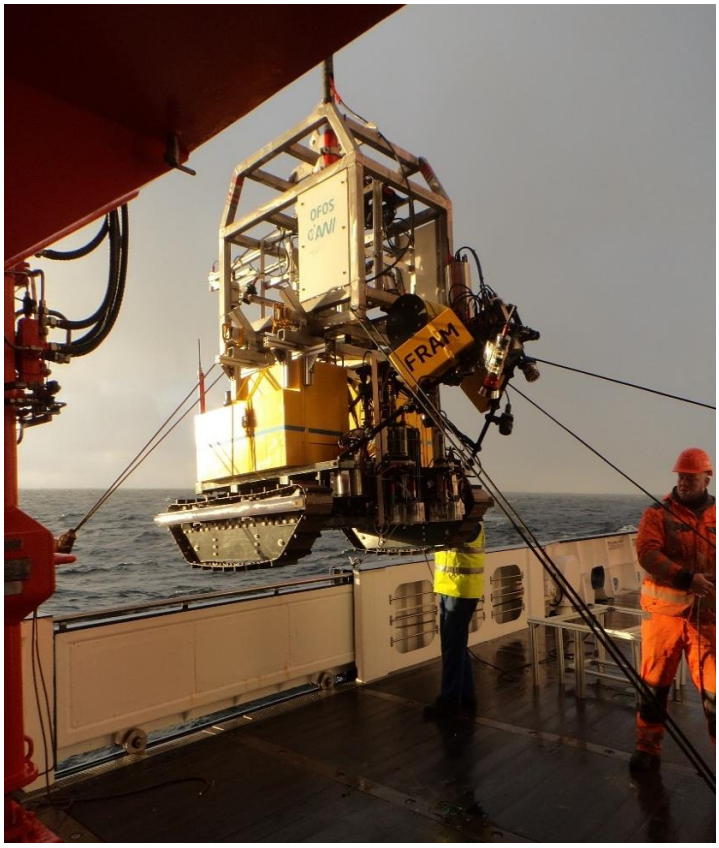


**Fig. 5.5.2** Deployment of NOMAD at HG-II using OFOS as launching system.

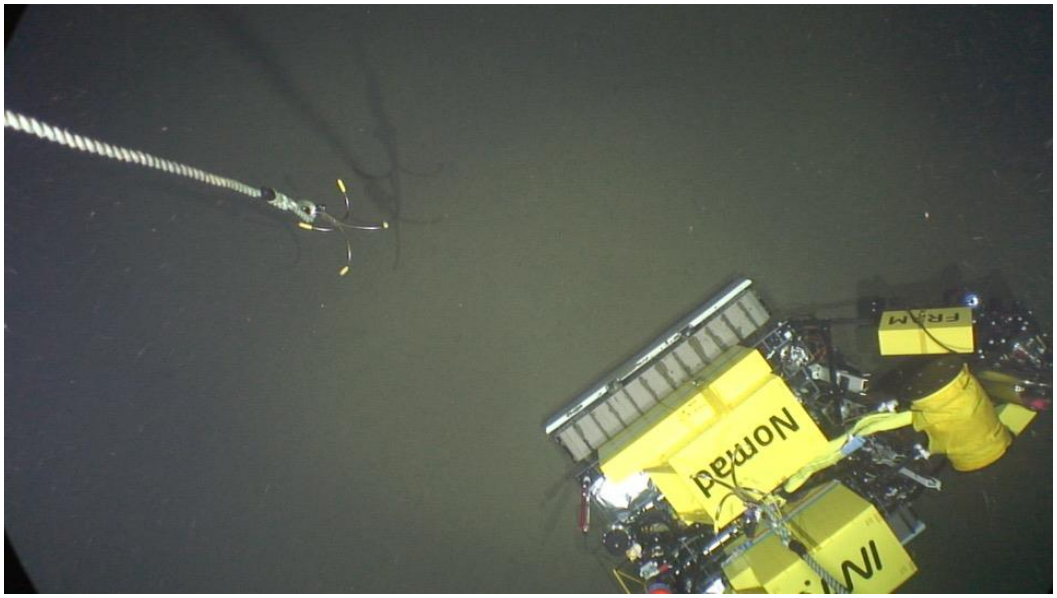


**Fig. 5.5.3** "Fishing" for NOMAD at 1550 m water depth using OFOS.

## 5.6 Experimental Work at the LTER Observatory HAUSGARTEN

(C. Hasemann, J. Hagemann, M. Hofbauer, U. Hoge, S. Lehmenhecker, T. Soltwedel)

Ocean acidification has been identified as a risk to marine ecosystems, and substantial scientific effort has been expended on investigating its effects, mostly in laboratory manipulation experiments. Experimental manipulations of $CO_2$ concentrations in the field are difficult, and the number of field studies are limited to a few locales. Within the EU project INTAROS (Integrated Arctic Observing System), the LTER observatory HAUSGARTEN was extended with an experimental system to study impacts of ocean acidification on benthic organisms and communities in deep Arctic waters with an autonomous system (Fig. 5.6.1). The so-called arcFOCE (Arctic Free Ocean Carbon Enrichment) system was developed to create semi-enclosed test areas on the seafloor where the seawater's pH (an indicator of acidity) can be precisely controlled for weeks or months at a time. The implementation of an arcFOCE for long-term experiments will enable us to generate data on the resistance of arctic marine benthic organisms and communities to a reduction in ocean pH. Before the long-term deployment of the bottom-lander-based arcFOCE system at 1500 m water depth in southern HAUSGARTEN area, we performed two short test deployment at the beginning of the cruise. After these successful test deployments, the system was re-deployed for one year with a several months operation time-period during the one-year deployment.

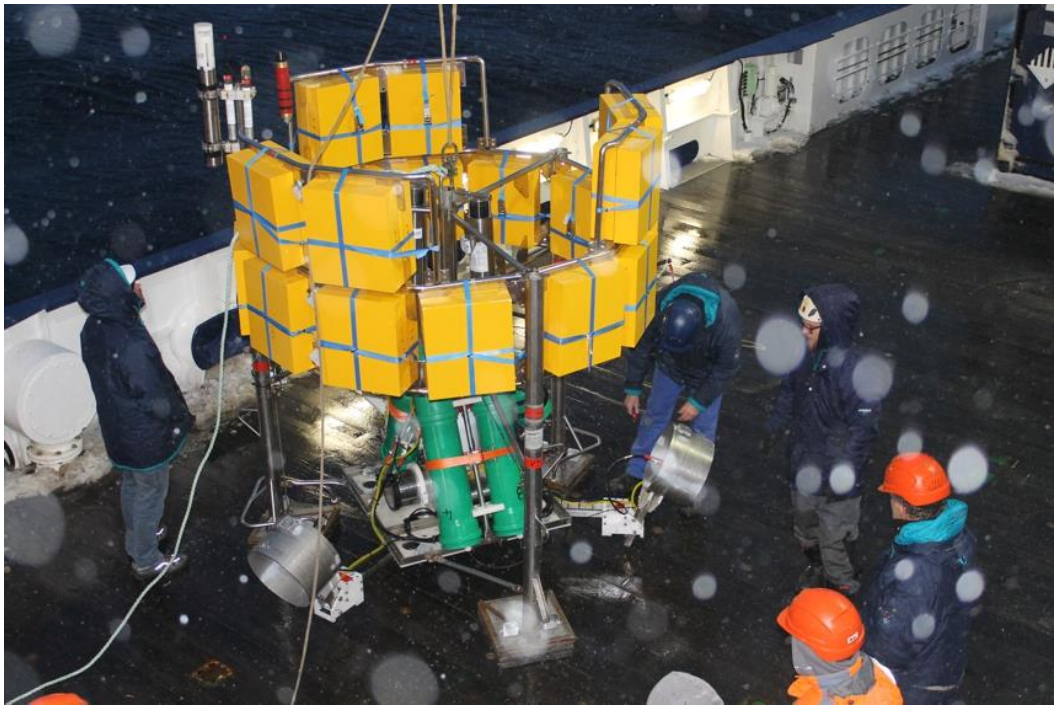

**Fig. 5.6.1** Preparing for the long-term deployment of the arcFOCE experimental set-up.

## 5.7 The FRAM Pollution Observatory: Marine Anthropogenic Litter and Microplastics in different Arctic Ecosystems

(M. Bergmann, M. Tekman)

Marine litter has long been on the political and public agenda, as it has been recognised as a rising pollution problem affecting all oceans and coastal areas of the world. There is currently a discrepancy of several orders of magnitude between estimates of global inputs of plastic litter, with figures derived from field measurements highlighting again the question: 'Where is all the plastic?'. Degradation of larger litter items into smaller particles termed 'microplastics' may be one reason for this discrepancy. Another possibility is that certain ecosystem compartments such as water column have not been considered so far with the latest research suggesting that the Arctic is an accumulation area for marine plastic. A newly added component to the open-ocean infrastructure FRAM (FRontiers in Arctic marine Monitoring) allows for the observation of marine litter and microplastics and other pollutants in different ecosystem compartments over long time scales.

The sampling campaign during MSM77 has aimed to collect samples from different marine compartments to answer these open questions. Four different sampling campaigns were executed during MSM77 to assess the spatial and temporal distribution of macrolitter and microplastic. Photographic surveys undertaken by a towed camera system (Ocean Floor Observation System, OFOS) were done to observe the change of the amount of macrolitter on the seafloor (Fig. 5.7.1). Analyses of OFOS images obtained previously at the LTER observatory HAUSGARTEN indicates a significant increase of litter on the seafloor between 2002 and 2014 (Bergmann & Klages, 2012; Tekman et al., 2017). Recent evidence suggests high concentrations of microplastics, a degradation product of larger plastic items, in Arctic marine sediments (Bergmann et al., 2017). The upper layer of the sediments was sampled with a video-guided multicorer for further analysis of microplastic particles. *In situ* pumps were deployed to get filtered water samples from different target depths of the water column. Litter was also recorded floating at the sea surface in the HAUSGARTEN area (Bergmann et al., 2015). Visual litter surveys were done to monitor the amount of floating marine litter.

- *Seafloor*

Three OFOS transects were executed at the HAUSGARTEN stations S3, HG-I, and HG-IV. 16 sediment samples were taken from multicorer deployments along the latitudinal and bathymetric transect (stations HG-IV, S3, SV-I, HG-IX, N5, N3) and frozen in tinfoil for assessments of microplastic concentrations.

**Fig. 5.7.1** Plastic bag "caught" by a dropstone at the deep seafloor off Svalbard (© M. Bergmann).

- *Water Column*

Two to four *In situ* pumps were deployed during deep CTD casts at six stations off East Greenland (EG-IV, D4) and off Svalbard (HG-I, HG-IV, HG-IX, N5, SV-I) at 2 to 4 depths (near surface, 300 m, 1000 m, near seafloor) of the water column. Between 200 L and 600 L of seawater were filtrated by one pump during 1 h of deployment.

- *Sea Surface*

A total of 17 neuston surveys of about 1 h duration were conducted to determine densities of floating litter when the ship was in transit to another station or to Edinburgh.

Floating litter was observed during 14 out of 17 transects. 35 of recorded items were plastic. The distribution of floating litter items was patchy but preliminary results showed that the transects with most items are concentrated in the central Fram Strait. Further analysis with µ-Fourier Transform InfraRed spectroscopy (µFTIR) is needed to assess microplastic amounts in sediments and *in situ* pump samples. Obvious litter items were observed during the OFOS transect at the central HAUSGARTEN station HG-IV. Possible litter items were recorded at all other sampling stations. Image analysis was completed on-board, detailed analysis is needed to obtain litter densities at each station.

# 6 Station List

| Station | Timestamp | Latitude | Longitude | Depth | Device |
|---|---|---|---|---|---|
| MSM77_1-1 | 16.09.2018 06:28 | 76°56.283'N | 14°59.959'E | 104 | Box Corer |
| MSM77_2-1 | 16.09.2018 13:44 | 77°49.998'N | 10°35.953'E | 144 | Box Corer |
| MSM77_3-1 | 16.09.2018 21:05 | 78°36.988'N | 05°04.081'E | 2292 | CTD |
| MSM77_3-2 | 16.09.2018 23:14 | 78°36.988'N | 05°04.079'E | 2293 | CTD |
| MSM77_3-3 | 17.09.2018 00:24 | 78°36.989'N | 05°04.083'E | 2292 | Marine Snow Catcher |
| MSM77_3-4 | 17.09.2018 01:25 | 78°36.989'N | 05°04.082'E | 2293 | Particle Camera |
| MSM77_3-5 | 17.09.2018 03:29 | 78°37.06'N | 05°00.069'E | 2313 | OFOS |
| MSM77_3-6 | 17.09.2018 08:38 | 78°37.441'N | 05°08.993'E | 2299 | Lander (Flux) |
| MSM77_4-1 | 17.09.2018 12:11 | 79°03.599'N | 04°09.532'E | 2448 | OFOS |
| MSM77_4-2 | 17.09.2018 15:15 | 79°03.595'N | 04°09.816'E | 2446 | Crawler (TRAMPER) |
| MSM77_4-3 | 17.09.2018 17:43 | 79°03.551'N | 04°12.013'E | 2431 | CTD |
| MSM77_4-4 | 17.09.2018 18:12 | 79°03.551'N | 04°12.014'E | 2432 | Marine Snow Catcher |
| MSM77_4-5 | 17.09.2018 19:03 | 79°03.551'N | 04°12.013'E | 2433 | In-situ Camera |
| MSM77_4-6 | 17.09.2018 20:27 | 79°03.551'N | 04°12.006'E | 2438 | CTD |
| MSM77_4-7 | 17.09.2018 22:29 | 79°03.914'N | 04°10.846'E | 2408 | Box Corer |
| MSM77_4-8 | 18.09.2018 01:28 | 79°03.914'N | 04°10.845'E | 2407 | Multi Corer |
| MSM77_4-9 | 18.09.2018 02:46 | 79°04.834'N | 04°06.759'E | 2439 | Lander (Long-term) |
| MSM77_4-10 | 19.09.2018 11:05 | 79°03.910'N | 04°18.437'E | 2346 | Drifting Trap |
| MSM77_4-11 | 18.09.2018 07:26 | 79°04.992'N | 04°05.545'E | 2445 | In-situ Camera |
| MSM77_5-1 | 18.09.2018 07:54 | 79°04.991'N | 04°05.541'E | 2446 | Litter Survey |
| MSM77_5-2 | 19.09.2018 12:55 | 79°04.025'N | 04°18.582'E | 2334 | Litter Survey |
| MSM77_5-3 | 19.09.2018 14:01 | 78°53.176'N | 04°40.353'E | 2735 | Litter Survey |
| MSM77_5-4 | 19.09.2018 15:07 | 78°40.901'N | 05°02.468'E | 2307 | Litter Survey |
| MSM77_5-5 | 20.09.2018 05:06 | 79°07.961'N | 06°07.084'E | 1238 | Litter Survey |
| MSM77_6-1 | 18.09.2018 09:23 | 79°03.601'N | 03°34.944'E | 3468 | CTD |
| MSM77_6-2 | 18.09.2018 10:32 | 79°03.601'N | 03°34.934'E | 3480 | AUV |
| MSM77_6-3 | 18.09.2018 18:17 | 79°03.609'N | 03°34.890'E | 3511 | Box Corer |
| MSM77_6-4 | 18.09.2018 21:08 | 79°03.609'N | 03°34.886'E | 3502 | Multi Corer |
| MSM77_7-1 | 19.09.2018 00:06 | 79°03.802'N | 03°39.499'E | 3085 | Box Corer |
| MSM77_7-2 | 19.09.2018 02:58 | 79°03.803'N | 03°39.497'E | 3092 | Multi Corer |
| MSM77_8-1 | 19.09.2018 05:16 | 79°06.483'N | 04°36.033'E | 1880 | CTD |
| MSM77_8-2 | 19.09.2018 06:27 | 79°06.491'N | 04°36.020'E | 1874 | Box Corer |
| MSM77_8-3 | 19.09.2018 08:52 | 79°06.491'N | 04°36.017'E | 1879 | Multi Corer |
| MSM77_9-1 | 19.09.2018 12:26 | 79°03.963'N | 04°18.444'E | 2338 | In-situ Camera |
| MSM77_10-1 | 19.09.2018 18:29 | 78°36.597'N | 05°04.119'E | 2289 | Box Corer |
| MSM77_10-2 | 19.09.2018 20:03 | 78°36.600'N | 05°04.111'E | 2289 | Multi Corer |
| MSM77_11-1 | 20.09.2018 01:07 | 79°07.933'N | 06°15.703'E | 1290 | OFOS |
| MSM77_12-1 | 20.09.2018 07:11 | 79°07.816'N | 04°54.162'E | 1510 | CTD |
| MSM77_12-2 | 20.09.2018 08:38 | 79°07.842'N | 04°54.167'E | 1508 | AUV |

| | | | | | |
|---|---|---|---|---|---|
| MSM77_12-3 | 20.09.2018 11:06 | 79°07.817'N | 04°54.074'E | 1510 | Box Corer |
| MSM77_12-4 | 20.09.2018 12:40 | 79°07.828'N | 04°54.114'E | 1508 | Multi Corer |
| MSM77_12-5 | 20.09.2018 14:38 | 79°08.011'N | 04°49.963'E | 1553 | Lander (arcFOCE) |
| MSM77_13-1 | 20.09.2018 16:11 | 79°08.002'N | 06°05.546'E | 1241 | CTD |
| MSM77_13-2 | 20.09.2018 16:42 | 79°08.004'N | 06°05.544'E | 1242 | Marine Snow Catcher |
| MSM77_13-3 | 20.09.2018 17:29 | 79°08.003'N | 06°05.547'E | 1247 | In-situ Camera |
| MSM77_13-4 | 20.09.2018 18:25 | 79°08.003'N | 06°05.546'E | 1246 | CTD |
| MSM77_13-5 | 20.09.2018 19:31 | 79°08.004'N | 06°05.544'E | 1242 | Box Corer |
| MSM77_13-6 | 20.09.2018 21:13 | 79°08.004'N | 06°05.545'E | 1243 | Multi Corer |
| MSM77_14-1 | 21.09.2018 01:21 | 78°36.602'N | 05°04.070'E | 2290 | Multi Corer |
| MSM77_15-1 | 21.09.2018 06:56 | 78°38.806'N | 09°27.864'E | 224 | MB Echosounder |
| MSM77_15-2 | 21.09.2018 09:16 | 78°39.174'N | 09°25.339'E | 237 | CTD |
| MSM77_15-3 | 21.09.2018 10:06 | 78°39.182'N | 09°25.297'E | 249 | AUV |
| MSM77_16-1 | 21.09.2018 20:32 | 79°00.003'N | 08°17.979'E | 818 | Box Corer |
| MSM77_17-1 | 21.09.2018 22:31 | 79°01.793'N | 06°59.666'E | 1266 | CTD |
| MSM77_17-2 | 21.09.2018 23:06 | 79°01.801'N | 06°59.886'E | 1266 | Marine Snow Catcher |
| MSM77_17-3 | 21.09.2018 23:21 | 79°01.807'N | 06°59.855'E | 1271 | Marine Snow Catcher |
| MSM77_17-4 | 22.09.2018 00:14 | 79°01.801'N | 06°59.890'E | 1267 | In-situ Camera |
| MSM77_17-5 | 22.09.2018 01:32 | 79°01.803'N | 06°59.896'E | 1269 | Box Corer |
| MSM77_17-6 | 22.09.2018 03:18 | 79°01.812'N | 06°59.930'E | 1270 | Multi Corer |
| MSM77_18-1 | 22.09.2018 08:45 | 79°07.503'N | 04°54.985'E | 1526 | Crawler (NOMAD) |
| MSM77_19-1 | 22.09.2018 13:02 | 78°59.995'N | 08°15.004'E | 870 | CTD |
| MSM77_20-1 | 22.09.2018 14:28 | 79°00.019'N | 08°42.067'E | 233 | AUV |
| MSM77_20-2 | 22.09.2018 17:02 | 79°00.011'N | 08°41.966'E | 231 | Box Corer |
| MSM77_20-3 | 22.09.2018 17:45 | 79°00.012'N | 08°41.963'E | 232 | Box Corer |
| MSM77_21-1 | 22.09.2018 18:38 | 79°00.003'N | 08°14.981'E | 871 | Drifting Trap |
| MSM77_21-2 | 22.09.2018 19:39 | 79°00.222'N | 08°16.847'E | 840 | Marine Snow Catcher |
| MSM77_21-3 | 22.09.2018 20:28 | 79°00.221'N | 08°16.849'E | 839 | In-situ Camera |
| MSM77_21-4 | 22.09.2018 21:45 | 79°00.233'N | 08°16.893'E | 840 | Multi Corer |
| MSM77_21-5 | 22.09.2018 22:35 | 79°00.231'N | 08°16.893'E | 841 | Multi Corer |
| MSM77_22-1 | 23.09.2018 00:22 | 78°58.809'N | 09°30.839'E | 222 | CTD |
| MSM77_22-2 | 23.09.2018 00:50 | 78°58.809'N | 09°30.839'E | 222 | Marine Snow Catcher |
| MSM77_22-3 | 23.09.2018 01:27 | 78°58.809'N | 09°30.843'E | 220 | In-situ Camera |
| MSM77_22-4 | 23.09.2018 02:01 | 78°58.836'N | 09°30.998'E | 220 | Multi Corer |
| MSM77_23-1 | 23.09.2018 03:02 | 79°00.016'N | 09°47.970'E | 224 | Box Corer |
| MSM77_24-1 | 23.09.2018 05:00 | 79°01.705'N | 11°05.172'E | 275 | CTD |
| MSM77_24-2 | 23.09.2018 07:39 | 79°01.702'N | 11°05.184'E | 278 | Multi Corer |
| MSM77_24-3 | 23.09.2018 08:19 | 79°01.705'N | 11°05.211'E | 277 | Multi Corer |
| MSM77_24-4 | 23.09.2018 09:09 | 79°01.704'N | 11°05.217'E | 278 | Box Corer |
| MSM77_25-1 | 23.09.2018 10:59 | 79°12.007'N | 11°53.974'E | 201 | Box Corer |
| MSM77_25-2 | 23.09.2018 11:28 | 79°12.007'N | 11°53.980'E | 202 | Box Corer |
| MSM77_26-1 | 23.09.2018 17:09 | 79°42.983'N | 09°54.956'E | 296 | Lander (Flux) |

| | | | | | |
|---|---|---|---|---|---|
| MSM77_27-1 | 23.09.2018 18:22 | 79°42.082'N | 010°0.066'E | 164 | In-situ Camera |
| MSM77_28-1 | 23.09.2018 21:37 | 79°56.491'N | 11°15.591'E | 130 | In-situ Camera |
| MSM77_29-1 | 24.09.2018 02:21 | 80°18.008'N | 13°59.951'E | 83 | CTD |
| MSM77_29-2 | 24.09.2018 02:49 | 80°18.007'N | 13°59.954'E | 82 | In-situ Camera |
| MSM77_29-3 | 24.09.2018 03:28 | 80°18.015'N | 13°59.952'E | 85 | Box Corer |
| MSM77_29-4 | 24.09.2018 08:39 | 80°18.019'N | 13°59.969'E | 83 | Box Corer |
| MSM77_30-1 | 24.09.2018 12:03 | 79°56.540'N | 11°16.277'E | 134 | Box Corer |
| MSM77_30-2 | 24.09.2018 12:57 | 79°56.538'N | 11°16.301'E | 134 | Box Corer |
| MSM77_31-1 | 24.09.2018 16:37 | 79°42.086'N | 10°00.075'E | 165 | Box Corer |
| MSM77_31-2 | 24.09.2018 17:54 | 79°42.087'N | 10°00.094'E | 164 | In-situ Camera |
| MSM77_32-1 | 24.09.2018 20:10 | 79°29.902'N | 08°41.704'E | 206 | Box Corer |
| MSM77_33-1 | 25.09.2018 15:12 | 79°08.012'N | 06°05.373'E | 1253 | In-situ Pump |
| MSM77_34-1 | 26.09.2018 14:51 | 78°59.151'N | 08°10.612'E | 940 | In-situ Camera |
| MSM77_35-1 | 27.09.2018 09:55 | 79°04.004'N | 04°10.093'E | 2415 | In-situ Camera |
| MSM77_35-2 | 27.09.2018 12:38 | 79°04.004'N | 04°10.067'E | 2418 | In-situ Pump |
| MSM77_35-3 | 27.09.2018 15:31 | 79°04.808'N | 04°06.772'E | 2438 | Lander (Long-term) |
| MSM77_35-4 | 27.09.2018 17:23 | 79°03.934'N | 04°17.377'E | 2354 | OFOS |
| MSM77_36-1 | 28.09.2018 00:12 | 79°03.788'N | 03°39.573'E | 3093 | CTD |
| MSM77_37-1 | 28.09.2018 01:04 | 79°03.610'N | 03°28.627'E | 4043 | CTD |
| MSM77_37-2 | 28.09.2018 04:01 | 79°03.617'N | 03°28.597'E | 4045 | Box Corer |
| MSM77_37-3 | 28.09.2018 07:16 | 79°03.631'N | 03°28.474'E | 4041 | Multi Corer |
| MSM77_38-1 | 28.09.2018 13:21 | 79°07.992'N | 02°50.538'E | 5551 | Drifting Trap |
| MSM77_38-2 | 28.09.2018 14:38 | 79°07.823'N | 02°49.554'E | 5552 | In-situ Camera |
| MSM77_38-3 | 28.09.2018 15:33 | 79°07.785'N | 02°49.584'E | 5549 | Lander (Flux) |
| MSM77_38-4 | 28.09.2018 17:47 | 79°08.015'N | 02°50.589'E | 5557 | Box Corer |
| MSM77_38-5 | 28.09.2018 21:04 | 79°08.039'N | 02°50.334'E | 5551 | Multi Corer |
| MSM77_38-6 | 29.09.2018 01:18 | 79°08.725'N | 02°55.163'E | 5543 | OFOS |
| MSM77_39-1 | 29.09.2018 11:48 | 79°06.781'N | 04°52.676'E | 1626 | AUV |
| MSM77_39-2 | 30.09.2018 13:18 | 79°07.690'N | 04°51.809'E | 1563 | Lander (arcFOCE) |
| MSM77_40-1 | 29.09.2018 18:15 | 79°03.869'N | 03°20.243'E | 5096 | CTD |
| MSM77_40-2 | 29.09.2018 20:16 | 79°03.866'N | 03°20.231'E | 5100 | Multi Corer |
| MSM77_41-1 | 30.09.2018 00:55 | 79°07.991'N | 02°49.754'E | 5555 | CTD |
| MSM77_41-2 | 30.09.2018 11:10 | 78°58.820'N | 03°29.119'E | 2510 | In-situ Camera |
| MSM77_42-1 | 30.09.2018 19:04 | 79°03.866'N | 03°20.222'E | 5121 | Box Corer |
| MSM77_43-1 | 30.09.2018 21:50 | 79°08.015'N | 02°50.598'E | 5573 | Marine Snow Catcher |
| MSM77_43-2 | 30.09.2018 22:06 | 79°08.015'N | 02°50.601'E | 5572 | Marine Snow Catcher |
| MSM77_44-1 | 01.10.2018 00:05 | 78°59.985'N | 01°30.078'E | 2527 | CTD |
| MSM77_44-2 | 01.10.2018 01:15 | 79°00.005'N | 01°30.024'E | 2527 | Box Corer |
| MSM77_44-3 | 01.10.2018 03:02 | 79°00.060'N | 01°29.963'E | 2527 | Multi Corer |
| MSM77_45-1 | 01.10.2018 12:29 | 78°38.718'N | 02°04.736'W | 2683 | CTD |
| MSM77_46-1 | 01.10.2018 16:11 | 78°32.948'N | 01°50.205'W | 2709 | In-situ Pump |
| MSM77_46-2 | 01.10.2018 16:54 | 78°32.948'N | 01°50.204'W | 2712 | In-situ Camera |

| | | | | | |
|---|---|---|---|---|---|
| MSM77_46-3 | 01.10.2018 18:48 | 78°32.951'N | 01°50.207'W | 2709 | In-situ Camera |
| MSM77_46-4 | 01.10.2018 19:48 | 78°32.959'N | 01°50.217'W | 2709 | CTD |
| MSM77_46-5 | 01.10.2018 21:03 | 78°32.960'N | 01°50.216'W | 2708 | Box Corer |
| MSM77_47-1 | 02.10.2018 02:42 | 78°45.002'N | 00°52.965'W | 2640 | CTD |
| MSM77_47-2 | 02.10.2018 03:53 | 78°45.005'N | 00°52.987'W | 2640 | Box Corer |
| MSM77_47-3 | 02.10.2018 05:40 | 78°45.027'N | 00°53.075'W | 2641 | Multi Corer |
| MSM77_48-1 | 02.10.2018 08:20 | 78°52.989'N | 00°18.039'E | 2544 | CTD |
| MSM77_48-2 | 02.10.2018 09:45 | 78°53.003'N | 00°18.050'E | 2543 | Box Corer |
| MSM77_48-3 | 02.10.2018 11:23 | 78°53.025'N | 00°17.975'E | 2550 | Multi Corer |
| MSM77_49-1 | 02.10.2018 15:10 | 79°19.360'N | 00°48.090'E | 3094 | CTD |
| MSM77_49-2 | 02.10.2018 16:18 | 79°22.123'N | 00°39.209'E | 3127 | CTD |
| MSM77_49-3 | 02.10.2018 17:23 | 79°25.004'N | 00°30.056'E | 3125 | CTD |
| MSM77_49-4 | 02.10.2018 17:54 | 79°25.608'N | 00°32.335'E | 3130 | CTD |
| MSM77_49-5 | 02.10.2018 18:30 | 79°26.267'N | 00°34.282'E | 3132 | CTD |
| MSM77_49-6 | 02.10.2018 19:15 | 79°26.890'N | 00°37.192'E | 3133 | CTD |
| MSM77_49-7 | 02.10.2018 19:47 | 79°27.517'N | 00°39.215'E | 3132 | CTD |
| MSM77_49-8 | 02.10.2018 20:21 | 79°28.208'N | 00°41.489'E | 3130 | CTD |
| MSM77_49-9 | 02.10.2018 20:52 | 79°28.865'N | 00°44.241'E | 3122 | CTD |
| MSM77_49-10 | 02.10.2018 21:24 | 79°29.596'N | 00°46.515'E | 3080 | CTD |
| MSM77_49-11 | 02.10.2018 22:00 | 79°30.226'N | 00°48.858'E | 3028 | CTD |
| MSM77_49-12 | 02.10.2018 22:42 | 79°30.895'N | 00°50.639'E | 2993 | CTD |
| MSM77_49-13 | 02.10.2018 23:29 | 79°31.576'N | 00°53.343'E | 2988 | CTD |
| MSM77_49-14 | 03.10.2018 00:10 | 79°32.307'N | 00°55.953'E | 3005 | CTD |
| MSM77_49-15 | 03.10.2018 00:45 | 79°32.975'N | 00°58.273'E | 3006 | CTD |
| MSM77_49-16 | 03.10.2018 01:25 | 79°33.617'N | 01°00.574'E | 2992 | CTD |
| MSM77_49-17 | 03.10.2018 02:01 | 79°34.273'N | 01°03.123'E | 2976 | CTD |
| MSM77_49-18 | 03.10.2018 02:43 | 79°34.935'N | 01°05.728'E | 2957 | CTD |
| MSM77_49-19 | 03.10.2018 03:50 | 79°35.459'N | 01°08.388'E | 2920 | CTD |
| MSM77_49-20 | 03.10.2018 04:30 | 79°36.135'N | 01°10.316'E | 2887 | CTD |
| MSM77_49-21 | 03.10.2018 05:10 | 79°36.889'N | 01°12.202'E | 2843 | CTD |
| MSM77_49-22 | 03.10.2018 05:46 | 79°37.521'N | 01°14.947'E | 2805 | CTD |
| MSM77_49-23 | 03.10.2018 06:24 | 79°38.256'N | 01°17.552'E | 2649 | CTD |
| MSM77_49-24 | 03.10.2018 07:08 | 79°38.935'N | 01°19.969'E | 2570 | CTD |
| MSM77_49-25 | 03.10.2018 07:42 | 79°39.618'N | 01°22.016'E | 2488 | CTD |
| MSM77_49-26 | 03.10.2018 08:36 | 79°40.213'N | 01°24.603'E | 2415 | CTD |
| MSM77_49-27 | 03.10.2018 09:19 | 79°40.895'N | 01°27.148'E | 2416 | CTD |
| MSM77_49-28 | 03.10.2018 09:57 | 79°41.547'N | 01°29.405'E | 2363 | CTD |
| MSM77_49-29 | 03.10.2018 10:35 | 79°42.214'N | 01°31.851'E | 2316 | CTD |
| MSM77_49-30 | 03.10.2018 11:16 | 79°42.878'N | 01°34.396'E | 2236 | CTD |
| MSM77_49-31 | 03.10.2018 11:54 | 79°43.574'N | 01°36.745'E | 2144 | CTD |
| MSM77_49-32 | 03.10.2018 12:34 | 79°44.238'N | 01°39.044'E | 2096 | CTD |
| MSM77_49-33 | 03.10.2018 13:10 | 79°44.923'N | 01°41.523'E | 2168 | CTD |

| | | | | | |
|---|---|---|---|---|---|
| MSM77_50-1 | 02.10.2018 15:27 | 79°19.372'N | 00°48.054'E | 3097 | ADCP |
| MSM77_51-1 | 03.10.2018 16:54 | 79°44.180'N | 04°29.040'E | 2620 | Drifting Trap |
| MSM77_52-1 | 03.10.2018 20:32 | 79°56.286'N | 03°11.646'E | 2494 | CTD |
| MSM77_52-2 | 03.10.2018 23:41 | 79°56.285'N | 03°11.766'E | 2496 | Marine Snow Catcher |
| MSM77_52-3 | 03.10.2018 23:57 | 79°56.285'N | 03°11.763'E | 2496 | Marine Snow Catcher |
| MSM77_52-4 | 04.10.2018 00:07 | 79°56.284'N | 03°11.761'E | 2497 | Marine Snow Catcher |
| MSM77_52-5 | 04.10.2018 01:04 | 79°56.284'N | 03°11.759'E | 2497 | In-situ Camera |
| MSM77_52-6 | 04.10.2018 03:13 | 79°56.284'N | 03°11.727'E | 2497 | Box Corer |
| MSM77_52-7 | 04.10.2018 05:26 | 79°56.296'N | 03°11.314'E | 2497 | Multi Corer |
| MSM77_53-1 | 04.10.2018 09:15 | 79°44.187'N | 04°29.117'E | 2619 | CTD |
| MSM77_53-2 | 04.10.2018 11:07 | 79°44.185'N | 04°29.110'E | 2623 | In-situ Camera |
| MSM77_53-3 | 04.10.2018 11:58 | 79°44.184'N | 04°29.110'E | 2616 | CTD |
| MSM77_53-4 | 04.10.2018 13:14 | 79°44.186'N | 04°29.120'E | 2616 | Box Corer |
| MSM77_53-5 | 04.10.2018 15:00 | 79°44.207'N | 04°29.021'E | 2619 | Multi Corer |
| MSM77_53-6 | 04.10.2018 17:55 | 79°39.069'N | 04°31.706'E | 3001 | In-situ Camera |
| MSM77_54-1 | 04.10.2018 19:18 | 79°36.230'N | 05°10.371'E | 2729 | CTD |
| MSM77_54-2 | 04.10.2018 20:03 | 79°36.233'N | 05°10.363'E | 2725 | Marine Snow Catcher |
| MSM77_54-3 | 04.10.2018 20:55 | 79°36.233'N | 05°10.358'E | 2729 | In-situ Camera |
| MSM77_54-4 | 04.10.2018 22:15 | 79°36.233'N | 05°10.370'E | 2727 | Box Corer |
| MSM77_54-5 | 05.10.2018 00:07 | 79°36.261'N | 05°10.326'E | 2727 | Multi Corer |
| MSM77_55-1 | 05.10.2018 08:46 | 79°07.502'N | 04°55.056'E | 1524 | OFOS |
| MSM77_55-2 | 05.10.2018 16:38 | 79°07.491'N | 04°54.918'E | 1530 | Lander (arcFOCE) |
| MSM77_56-1 | 05.10.2018 17:48 | 79°03.622'N | 04°07.623'E | 2475 | Crawler (TRAMPER) |
| MSM77_56-2 | 05.10.2018 18:07 | 79°03.623'N | 04°07.627'E | 2477 | Marine Snow Catcher |
| MSM77_57-1 | 06.10.2018 04:13 | 79°01.312'N | 10°50.956'E | 321 | In-situ Camera |
| MSM77_57-2 | 06.10.2018 05:19 | 79°01.312'N | 10°50.956'E | 321 | In-situ Camera |
| MSM77_58-1 | 06.10.2018 07:26 | 79°01.070'N | 11°30.250'E | 278 | AUV |

## 7 Data and Sample Storage and Availability

Samples will be processed and stored at AWI and GEOMAR. All OFOS images, videos and metadata will be uploaded to PANGAEA as will be data on microplastic concentration. These data will also be uploaded to the online portal 'LITTERBASE' (www.litterbase.org). Data acquisition from the several types of investigation will be differently time-consuming. The time period from post processing to data provision will vary from one year maximum for sensor data, to several years for organism related datasets. Until then preliminary data will be available to the cruise participants and external users after request to the senior scientist. The finally processed data will be submitted to the PANGAEA data library. The unrestricted availability from PANGAEA will depend on the required time and effort for acquisition of individual datasets and its status of scientific publication. Data will preferably be published in open access journals.

## 8 Acknowledgements

We would like to thank Captain Ralf Schmidt and his crew for their hospitality, trusting collaboration and the great atmosphere on board. Financial support for the cruise was provided through the AWI – Research-Program PACES-II (Polar Regions and Coasts in the changing Earth System) as well as through funding by the research institutes involved. We gratefully acknowledge this support.

## 9 References

AMAP, 2013. AMAP Assessment 2013: Arctic Ocean Acidification. Arctic Monitoring and Assessment Programme, Oslo, Norway. viii + 99 pp.

Arrigo, K.R., 2013. The changing Arctic Ocean. Elem. Sci. Anth. 1, doi:10.12952/journal. elementa.000010.

Bates, N.R., Mathis, T., Cooper, L.W., 2009. Ocean acidification and biologically induced seasonality of carbonate mineral saturation states in the western Arctic Ocean. J. Geophys. Res. 114, C11007, doi:10.1029/2008JC004862.

Bergmann, M., Soltwedel, T., Klages, M., 2011. The interannual variability of megafaunal assemblages in the Arctic deep sea: Preliminary results from the HAUSGARTEN observatory (79°N). Deep-Sea Res. I 58(6), 711-723.

Bergmann, M., Klages, M., 2012. Increase of litter at the Arctic deep-sea observatory HAUSGARTEN. Mar. Pollut. Bull. 64(12), 2734-2741.

Bergmann, M., Sandhop, N., Schewe, I., D'Hert, D., 2015. Observations of floating anthropogenic litter in the Barents Sea and Fram Strait, Arctic. Pol. Biol. 39(3), 553-560.

Bergmann, M., Wirzberger, V., Krumpen, T., Lorenz, C., Primpke, S., Tekman, M.B., Gerdts, G., 2017. High Quantities of Microplastic in Arctic Deep-Sea Sediments from the HAUSGARTEN Observatory. Environ. Sci. Technol. 51(19), 11000-11010. doi: 10.1021/acs.est.7b03331.

Budaeva, N.E., Mokievsky, V.O., Soltwedel, T., Gebruk, A.V., 2008. Horizontal distribution patterns in Arctic deep-sea macrobenthic communities. Deep-Sea Res. I 55(9), 1167-1178.

Burrows, M.T., Schoeman, D.S., Buckley, L.B., Moore, P., Poloczanska, E.S., Brander, K.M., Brown, C., Bruno, J.F., Duarte, C.M., Halpern, B.S., Holding, J., Kappel, C.V., Kiessling, W., O'Connor, M.I., Pandolfi, J.M., Parmesan, C., Schwing, F.B., Sydeman, W.J., Richardson, A.J., 2011. The pace of shifting climate in marine and terrestrial ecosystems. Science 334(6056), 652-655.

Burrows, M.T., Schoeman, D.S., Richardson, A.J., Molinos, J.G., Hoffmann, A., Buckley, L.B., Moore, P.J., Brown, C.J., Bruno, J.F., Duarte, C.M., Halpern, B.S., Hoegh-Guldberg, O., Kappel, C.V., Kiessling, W., O'Connor, M.I., Pandolfi, J.M., Parmesan, C., Sydeman, W.J., Ferrier, S., Williams, K.J., Poloczanska, E.S., 2014. Geographical limits to species-range shifts are suggested by climate velocity. Nature 507, 492-495.

Caron, D.A., Hutchins, D.A., 2013. The effects of changing climate on microzooplankton grazing and community structure: drivers, predictions and knowledge gaps. J. Plankton Res. 35(2), 235-252.

Comiso, J.C., Parkinson, C.L., Gersten, R., Stock, L., 2008. Accelerated decline in the Arctic sea ice cover. Geophys. Res. Lett. 35, L01703, doi:10.1029/2007GL031972.

Engel, A. et al., 2013. CO2 increases 14C primary production in an Arctic plankton community. Biogeosciences 10, 1291-1308.

Engel, A., Piontek, J., Metfie,s K., Endres, S., Sprong, P., Peeken, I., Gäbler-Schwarz, S., Nöthig, E.-M., 2017. Inter-annual variability of transparent exopolymer particles in the Arctic Ocean reveals high sensitivity to ecosystem changes. Sci. Rep. 7(4129), 1-9.

Fadeev, E., Salter, I., Schourup-Kristensen, V., Metfies, K., Engel, A., Piontek, J., Nöthig, E.-M., Boetius, A., Bienhold, C. (*under review*). Microbial communities in the East and West Fram Strait during sea-ice melting season. Front. Mar. Sci.

Gallucci, F., Fonseca, G., Soltwedel, T., 2008. Effects of megafauna exclusion on nematode assemblages at a deep-sea site. Deep-Sea Res. I 55(3), 332-349.

Grassle, J.F., Sanders, H.L., Hessler, R.R., Rowe, G.T., McLellan, T., 1975. Pattern and zonation: a study of the bathyal megafauna using the research submersible Alvin. Deep-Sea Res. Oceanogr. Abstr. 22(7), 457-462.

Guilini, K., Soltwedel, T., van Oevelen, D., Vanreusel, A., 2011. Deep-sea nematodes actively colonise sediments, irrespective of the presence of a pulse of organic matter: Results from an in situ experiment. PLoS One 6(4), e18912.

Hassol, S.J., 2004. ACIA, Impacts of a warming Arctic: Arctic climate impact assessment. Cambridge University Press.

Hirche, H.J., Kosobokova K., 2007. Distribution of *Calanus finmarchicus* in the northern North Atlantic and Arctic Ocean – Expatriation and potential colonization. Deep-Sea Res. II, 2,729-2,747.

IPCC, 2013. Climate Change 2013: The Physical Science Basis. Contribution of Working Group I to the Fifth Assessment Report of the Intergovernmental Panel on Climate Change [Stocker, T.F., Qin, D., Plattner, G.-K., Tignor, M., Allen, S.K., Boschung, J., Nauels, A., Xia, Y., Bex, V., Midgley, P.M. (Eds.)], Cambridge University Press, Cambridge, United Kingdom and New York, NY, USA, 1535 pp.

Jones, D.O.B., Yool, A., Wei, C.-L., Henson, S.A., Ruhl, H.A., Watson, R.A., Gehlen, M., 2013. Global reductions in seafloor biomass in response to climate change. Glob. Change Biol. 20(6), 1861-1872.

Käß, M., Vedenin, A., Hasemann, C., Brandt, A., Soltwedel, T., (*in prep.*). Community structure of macrofauna in the deep Fram Strait: A comparison between two bathymetric gradients in ice covered and ice free areas.

Kanzog, C., Ramette, A., Quéric, N.V., Klages, M., 2009. Response of benthic microbial communities to chitin enrichment: an in situ study in the deep Arctic Ocean. Polar Biol. 32, 105-112.

Kortsch, S., Primicerio, R., Beuchel, F., Renaud, P.E., Rodrigez, J., Lønne, O.J., Gulliksen, B., 2012. Climate-driven regime shifts in Arctic marine benthos. Proc. Natl. Acad. Sci. USA 109(35), 14052-14057.

Lischka, S., Riebesell, U., 2012. Synergistic effects of ocean acidification and warming on overwintering pteropods in the Arctic. Glob. Change Biol. 18(12), 3,517-3,528.

Metfies, K., von Appen, W.J., Kilias, E., Nicolaus, A., Nöthig, E.-M., 2016. Biogeography and Photosynthetic Biomass of Arctic Marine Pico-Eukaryotes during Summer of the Record Sea Ice Minimum 2012. PLoS One, 11(2), e0148512.

Meyer, K., Bergmann, M., Soltwedel, T., 2013. Interannual variation in the epibenthic megafauna at the shallowest station of the HAUSGARTEN observatory (79°N, 6°E). Biogeosciences 10, 3479-3492.

Nöthig, E.-M., Bracher, A., Engel, A., Metfies, K., Niehoff, B., Peeken, I., Bauerfeind, E., Cherkasheva, A., Gäbler-Schwarz, S., Hardge, K., Kilias, E., Kraft, A., Mebrahtom Kidane, Y., Lalande, C., Piontek, J., Thomisch, K., Wurst, M., 2015. Summertime plankton ecology in Fram Strait - a compilation of long- and short-term observations. Pol. Res. 34, doi:10.3402/polar.v34.23349.

Parkinson, C.L., Cavalieri, D.J., Gloersen, P., Zwally, H.J., Comiso, J.C., 1999. Arctic sea ice extents, areas, and trends, 1978-1996. J. Geophys. Res. 104(C9), 20837-20856.

Poloczanska, E.S., Brown, C.J., Sydeman, W.J., Kiessling, W., Schoeman, D.S., Moore, P.J., Brander, K., Bruno, J.F., Buckley, L.B., Burrows, M.T., Duarte, C.M., Halpern, B.S., Holding, J., Kappel, C.V., O'Connor, M.I., Pandolfi, J.M., Parmesan, C., Schwing, F., Thompson, S.A., Richardson, A.J., 2013. Global imprint of climate change on marine life. Nat. Clim. Change 3, 919-925.

Premke, K., Klages, M., Arntz, W.E., 2006. Aggregations of Arctic deep-sea scavengers at large food falls: temporal distribution, consumption rates and population structure. Mar. Ecol. Prog. Ser. 325, 121-135.

Rex, M.A., 1981. Community structure in the deep-sea benthos. Annu. Rev. Ecol. Syst. 12, 331-353.

Simon, M., Azam, F., 1989. Protein content and protein synthesis rates of planktonic marine bacteria. Mar. Ecol. Prog. Ser. 51, 201-213.

Soltwedel, T., Bauerfeind, E., Bergmann, M., Budaeva, N., Hoste, E., Jaeckisch, N., Juterzenka, K. v., Matthießen, J., Mokievsky, V., Nöthig, E.-M., Quéric, N., Sablotny, B., Sauter, E., Schewe, I., Urban-Malinga, B., Wegner, J., Włodarska-Kowalczuk, M., Klages, M., 2005. HAUSGARTEN: multidisciplinary investigations at a deep-sea, long-term observatory in the Arctic Ocean. Oceanogr. 18(3), 46-61.

Soltwedel, T., Volkenandt, M., Mokievsky, V., Hasemann, C., Sauter, E., Rabouille, C., 2013. Effects of experimentally increased near-bottom flow on meiofauna diversity in the deep Arctic Ocean. Deep-Sea Res. I 73, 31-45.

Soltwedel, T., Bauerfeind, E., Bergmann, M., Bracher, A., Budaeva, N., Busch, K., Cherkasheva, A., Fahl, K., Grzelak, K., Hasemann, C., Jacob, M., Kraft, A., Lalande, C., Metfies, K., Nöthig, E.-M., Meyer, K., Quéric, N.V., Schewe, I., Włodarska-Kowalczuk, M., Klages, M., 2016. Natural variability or anthropogenically induced variation? Insights from 15 years of multidisciplinary observations at the arctic open ocean LTER site HAUSGARTEN. Ecol. Ind. 65, 89-102.

Soltwedel, T., Guilini, K., Sauter, E., Schewe, I., Hasemann, C., 2017. Local effects of large food falls on nematode diversity at an arctic deep sea site: Results from an in situ experiment at the LTER observatory HAUSGARTEN. J. Exp. Mar. Biol. Ecol. 502, 129-141.

Taylor, J., Krumpen, T., Soltwedel, T., Gutt, J., Bergmann, M., 2017. Dynamic benthic megafaunal communities: Assessing temporal variations in structure, composition and diversity at the Arctic deep-sea observatory HAUSGARTEN between 2004 and 2015. Deep-Sea Res. I 122, 81-94.

Taylor, J., Staufenbiel, B., Soltwedel, T., Bergmann, M., 2018. Temporal trends in the biomass of three epibenthic invertebrates from the deep-sea observatory HAUSGARTEN (Fram Strait, Arctic Ocean). Mar. Ecol. Prog. Ser. 602, 15-29.

Tekman, M.B., Krumpen, T., Bergmann, M., 2017. Marine litter on deep Arctic seafloor continues to increase and spreads to the North at the HAUSGARTEN observatory. Deep-Sea Res. I 120, 88-99.

Vedenin, A., Budaeva, N., Mokievsky, V., Pantke, C., Soltwedel, T., Gebruk, A., 2016. Spatial distribution patterns in macrobenthos along a latitudinal transect at the deep-sea observatory HAUSGARTEN. Deep-Sea Res. I 114, 90-98.

Wassmann, P., Duarte, C.M., Agusti, S., Sejr, M.K., 2011. Footprints of climate change in the Arctic marine ecosystem. Glob. Change Biol. 17, 1235-1249.

Wlodarska-Kowalczuk, M., Kendall, M.A., Weslawski, J.M., Klages, M., Soltwedel, T., 2004. Depth gradients of benthic standing stock and diversity on the continental margin at a high-latitude ice-free site (off Spitsbergen, 79 N). Deep-Sea Res. I 51(12), 1903-1914.

Wohlers, J., Engel, A., Zöllner, E., Breithaupt, P., Jürgens, K., Hoppe, H.-G., Sommer, U., Riebesell, U., 2009. Changes in biogenic carbon flow in response to sea surface warming. Proc. Natl. Acad. Sci. 106, 7067-7072.